

Yuxin Shi, Puxuan Lu, Yuxin Yang, Chunhong Hu,
Haiying Jin, and Lili Kong

11.1 Introduction

11.1.1 Definition and Prevalence

Human infected H7N9 avian influenza is an acute respiratory infectious disease caused by subtype H7N9 of avian influenza virus. Since the first case was reported in Yangzi River Delta of China in Feb. 2013, the total cases with definitive diagnosis had been up to 451 cases, including 176 cases of death, by Dec. 31, 2014, with a mortality rate of roughly 39 %.

11.1.2 Epidemiology

11.1.2.1 Source of Infection

Currently, subtype H7N9 of avian influenza virus has been isolated from the secretions and excretions of poultry, which is highly homologous with human infected H7N9 avian influenza virus. The source of its infection may be poultry carrying H7N9 avian influenza virus. And no defi-

nite evidence has been found supporting interpersonal transmission of H7N9 avian influenza virus, but its limited continual transmission from person to person has not been excluded.

11.1.2.2 Route of Transmission

Human is infected via respiratory tract. And close contact to excretions or secretions of infected poultry and direct contact to the virus can also cause its infection.

11.1.2.3 Susceptible Population

Individuals who have a history of contact to poultry within 1 week prior to onset are high risk population, such as those engaging in poultry raising, selling, slaughtering and processing.

11.1.3 Clinical Manifestation

The patients commonly experience influenza like symptoms, such as fever, cough with a little sputum, accompanying headache, muscle soreness and general malaise. In severe cases, the condition rapidly progresses, commonly into severe pneumonia within 5–7 days and the body temperature mostly above 39 °C, with dyspnea and accompanying bloody sputum. The condition may rapidly develop into acute respiratory distress syndrome (ARDS), sepsis, septic shock, and even multiple organs failure. Some patients may also develop mediastinal emphysema and pleural effusion. And its incubation period generally lasts for no more than 7 days.

11.1.4 Laboratory Test

11.1.4.1 Routine Blood Test

Generally, the WBC count may decrease. In severe cases, WBC count and lymphocyte count commonly decrease, possibly with decreased platelets.

Y. Shi (✉)
Affiliated Clinical Center of Public Health, Fudan University,
Shanghai, China
e-mail: shiyx828288@163.com

P. Lu
Affiliated Shenzhen Third People's Hospital,
Guangdong Medical College, Shenzhen, Guangdong, China

Y. Yang
Xinjiang Sixth People's Hospital, Urumuqi, Xinjiang, China

C. Hu
Affiliated First Hospital, Suzhou University,
Suzhou, Jiangsu, China

H. Jin
Affiliated Huaihe Hospital, Henan University,
Kaifeng, Henan, China

L. Kong
Yeda Hospital, Yantai, Shandong, China

11.1.4.2 Blood Biochemistry

By blood biochemistry, the levels of creatine kinase, lactic dehydrogenase, aspartate amino transferase, alanine amino-transferase show increases. And C reactive protein level increases, possibly with increase of myohemoglobin level.

11.1.4.3 Etiological and Related Examination

Before anti-viral therapy is prescribed, it is necessary to collect the respiratory secretions for examination, such as nasopharyngeal secretions, oral gargle, tracheal aspirates or respiratory epithelial cells. In well equipped hospitals, the etiological examination should be performed immediately; while in poorly equipped hospitals, the specimen should be sent to entrusted institutions for etiological examination.

Antigen Screen of Influenza A Virus

Rapid detection for the antigen of influenza A virus in respiratory specimens can only be used for primary screening of human infected H7N9 avian influenza.

Nucleic Acid Test

PCR can be perform to examine respiratory secretions for subtype H7N9 of avian influenza virus.

Virus Isolation

The subtype H7N9 of avian influenza virus can be isolated from specimens of respiratory secretions.

Dynamic Detection of Paired Sera

In the patients with human infected H7N9 avian influenza virus, the specific antibody of H7N9 avian influenza virus increases at least 4 times.

11.1.5 Chest Radiology

Clinically, human infected H7N9 avian influenza can be categorized into 3 types, namely asymptomatic (latent infection), slight and severe. In the hospital we work in, 18 patients were hospitalized, with 1 case of slight infection and 17 cases of severe infection. The patient with slight infection only experienced flue like symptoms, such as fever, but no lung abnormality. However, the 17 patients with severe infection experienced severe pneumonia, with the conditions

meeting the diagnostic criteria of severe pneumonia induced by H7N9 avian influenza virus issued by National Health and Family Planning Commission. The clinical manifestations of severe pneumonia induced by human infected H7N9 avian influenza are as the following:

11.1.5.1 Early Stage

The early lesions are mainly located in lower lobe of one lung, predominantly with a segmental distribution. Radiologically, they are ground glass opacity, interlobular septal thickening and acinar nodules.

11.1.5.2 Progressive Stage

The pulmonary lesions progresses rapidly from small flakes of opacity to large consolidations, from one segment to multiple segments, from one lung to both lungs, and from lower lobes to the whole lungs. Within 24–48 h, the pulmonary lesions may spread rapidly to involve multiple lobes of both lungs. In severe cases, the pulmonary lesions show a significant increase ($\geq 50\%$) within several hours. The lesions develop rapidly from ground glass opacity to consolidation opacity, and the density of consolidation opacity increases, with occurrence of serous effusion. The pulmonary lesions commonly reach their peak within 5–0 days, with observable lung air sac at this time.

11.1.5.3 Convalescent Stage

For the cases with no complication, if prompt anti-viral therapy administered, the lesions begin to be absorbed slowly after their reaching the peak, firstly the ground glass opacity, and then consolidations and the lesions in the central area adjacent to the hilum. The consolidations show decreasing density to sparse and the consolidated lung tissues gradually inflate. During the whole process of absorption, the lesions in middle and upper lung lobes are absorbed earlier than the lesions in dorsal lower lung lobes and the subpleural lesions. The early lesions that emerge during the early and progressive stages are absorbed late, and the lesions that emerge late are firstly absorbed. Radiologically, pulmonary fibrosis is demonstrated as small patches, fibrous cords like, grid like, and small ground glass opacity in subpleural areas of both lungs and/or dorsal segments of both lower lungs. Meanwhile, subpleural paraseptal emphysema, scar type emphysema, subpleural lung bullae and limited bronchiectasis are revealed.

11.2 Typical Cases

Case 1

[Brief Case History]

A 53-year-old man of Han nationality complained of intermittent fever for 13 days and difficulty breathing for 4 days that aggravated as well as unconsciousness for 2 h. After ineffective treatment in another hospital, he was transferred to our hospital on Aug. 16, 2014. Laboratory tests showed nucleic acid of H7N9 avian influenza virus positive, with increased neutrophils and decreased lymphocytes. Blood biochemistry revealed increased levels of γ -glutamyl transpeptidase, lactate dehydrogenase and α -hydrobutyrate dehydrogenase. During hospitalization for treatment, he received bed-side chest DR radiography per day (totally 8 bed-side chest DR films and 3 chest CT scans) to assess his conditions. After emergency rescuing, he was cured and discharged on Sep. 5, 2014. After that, he received 2 follow-up chest CT scans for re-examination.

[Radiological demonstration] Fig. 11.1

[Diagnosis] Pneumonia induced by human infected H7N9 avian influenza virus, severe pneumonia, and ARDS.

[Discussion]

Pneumonia induced by human infected H7N9 avian influenza is an acute respiratory infectious disease caused by subtype H7N9 of avian influenza virus and it occurs in any age group of people. Before onset, the patient usually has a history of exposure to an environment contaminated by avian influenza virus, and the common clinical manifestations include cough, expectoration, and fever. The condition progresses rapidly in seriously ill patients, with occurrence of severe pneumonia within 3–7 days after onset. The body temperature mostly persists above 39 °C with dyspnea, which rapidly further progresses into acute respiratory distress syndrome (ARDS), sepsis, septic shock, and even multiple organs failure.

Pneumonia induced by human infected H7N9 avian influenza is radiologically characterized by the following:

1. Morphologically, the lesions are pulmonary consolidation, ground glass opacity and interstitial changes.

2. The lesions are diffusely distributed in both lungs in severe cases, which are more serious in lower lungs.
3. The lesions show rapid progression, with emergence or increase of consolidations during the progressive stage.
4. The primary ground glass opacity in lungs shows obvious consolidation inside within a short period of time. Otherwise, the range with primary consolidations enlarges with increased density.
5. The lesions are migratory, with absorption of primary lesions within a short period of time and newly emerging lesions in other parts of lungs, which are radiologically characteristic.
6. The lesions show slow absorption, with signs of pulmonary fibrosis after cured.
7. Chest CT demonstrations are inconsistent to the clinical symptoms because the absorption of lesions lags behind. Re-examination by chest CT scan show slight absorption of the lung lesions after the clinical symptoms are obviously improved.

Pneumonia induced by human infected H7N9 avian influenza should be differentiated from the following diseases:

1. Pneumonia induced by influenza virus
Its occurrence is related to prevalence of influenza, with rapid progression. Radiologically, the lesions are mainly confined and segmental alveolar consolidation, which may further develop into diffuse lesions with air bronchogram. By chest X-ray, it shares commonalities with pneumonia induced by H7N9 avian influenza, and their differential diagnosis is challenging. And its final definitive diagnosis should be based on the laboratory tests.
2. Adenoviral pneumonia
It is more common in children whose chest X-ray demonstrations include increased, thickened and blurry lung markings. The lesions distribute extensively,

Fig. 11.1 Chest X-ray demonstrated consolidation and ground glass opacity in the right upper lung and the left lower lung, with uneven density, poorly defined boundary, and inner air bronchogram (a). Re-examination after 4 days demonstrated consolidation and ground glass opacity in the right upper lung and the left lower lung, with decreased density and smaller lesion range (b). Re-examination after 6 days showed consolidation and ground glass opacity in the right upper lung and the left lower lung, with further decreased density and smaller lesion range (c). Re-examination after 12 days revealed consolidation and ground glass opacity in the right upper

lung and the left lower lung, with further decreased density and smaller lesion range; and partially interstitial fibrosis (d). Re-examination by chest CT scan after 36 days demonstrated multiple small patches of dense opacity in both lungs and in lateral part of lungs, predominantly in the right upper lung and the left lower lung, and partially interstitial fibrosis (e, f). Re-examination by chest CT scan after 5 months demonstrated obviously decreased small patches of dense opacity in both lungs, with rare fibrous cords like opacity (g)

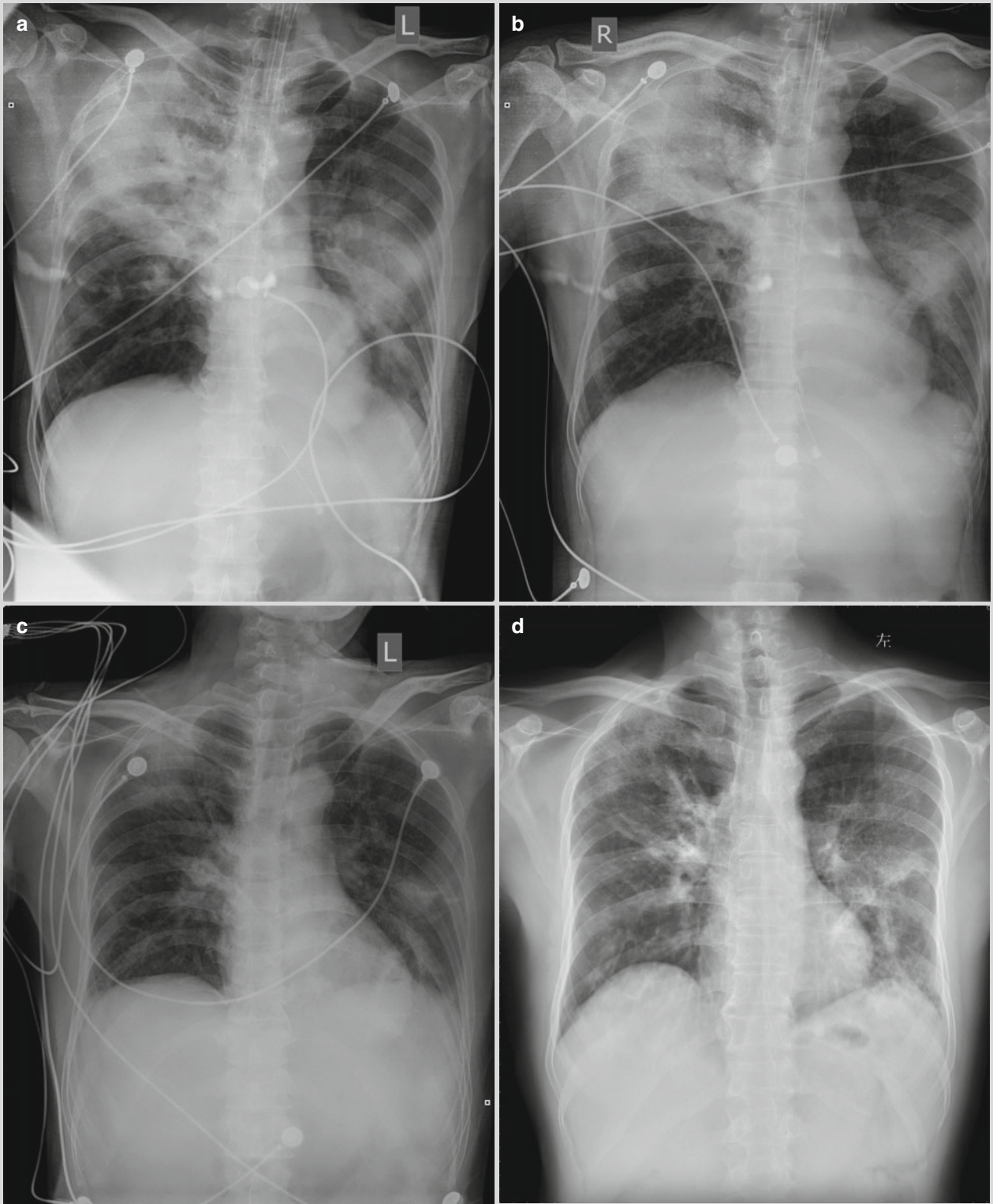


Fig.11.1 (continued)

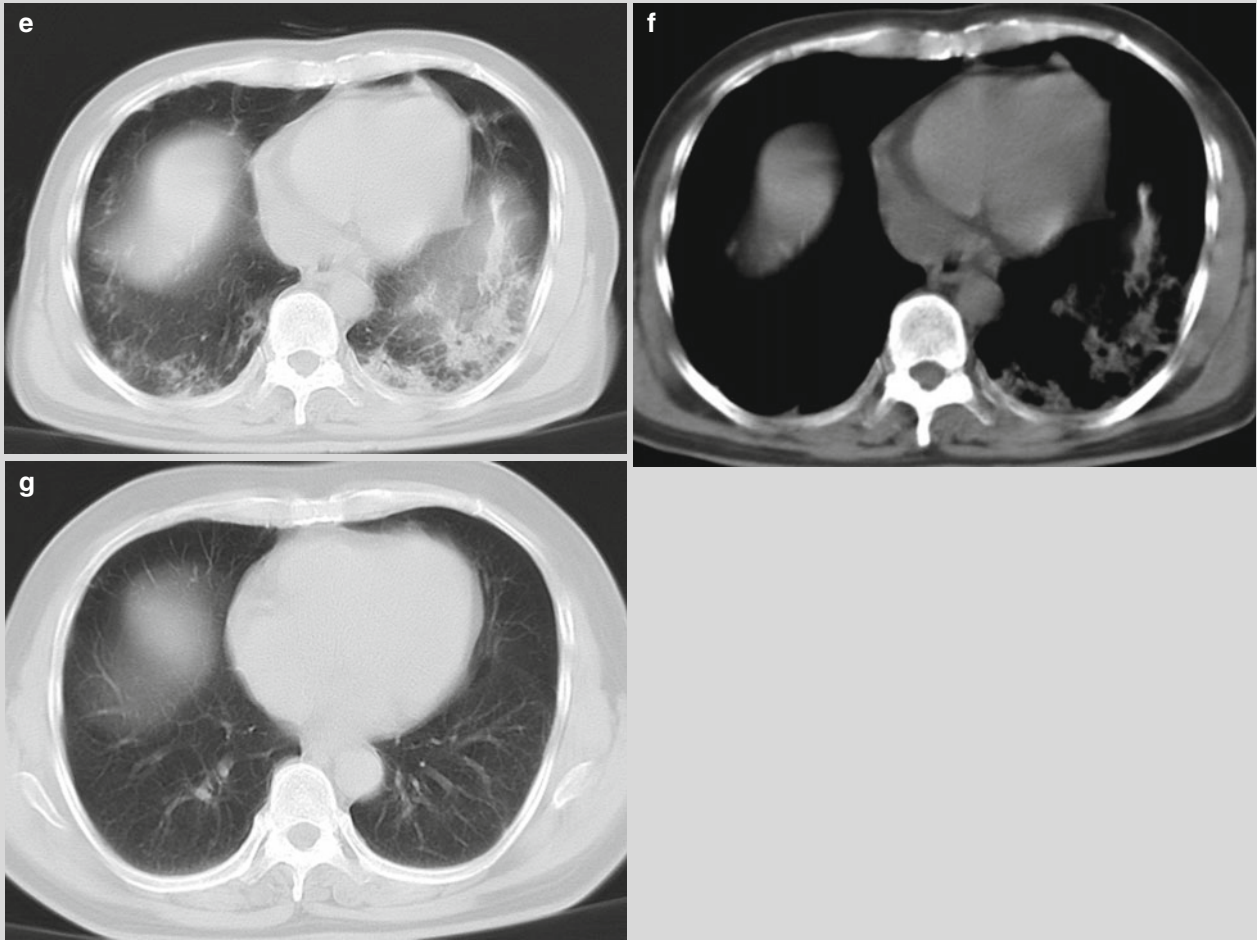


Fig.11.1 (continued)

which are characterized by many lung markings, many lesions of emphysema, many integrated lesions and many large lesions, but rare round lesions, rare lesions of lung bullae and rare pleural effusion as well as consistency between radiological signs and clinical symptoms.

3. Severe acute respiratory syndrome (SARS)

The patients with SARS have definite epidemiological history of contact. By chest X-ray, it is demonstrated with diversifying lesions, among which cotton like exudation is the most common; multi-focus granuloma and false cavity are possibly its specific signs.

Case 2

[Brief Case History]

A 65-year-old man of Han Chinese, experienced cough, expectoration, obvious increase of the body temperature, dyspnea, tachypnea, chest distress and shortness of breath. By CT scan in another hospital, inflammation of both lungs and bilateral pleural effusion were revealed. He was transferred into our hospital on Dec. 12, 2014. Laboratory tests showed the nucleic acid of H7N9 avian influenza virus positive; neutrophils within normal range, decreased lymphocytes count; increased levels of γ -glutamyl transpeptidase, lactate dehydrogenase, α -hydrobutyrate dehydrogenase, serum lipoprotein, and C reactive protein; increased creatinine level that exceeded the normal range as well as increased levels of creatinine and cystatin C. Bedside chest DR radiography per day (totally 5 chest DR films) in our hospital was ordered to monitor the lesion changes. Death finally occurred on Dec. 16, 2014 due to multiple organs failure after ineffective emergency rescuing.

[Radiological demonstration] Fig. 11.2

[Diagnosis] Critical case of human infected H7N9 avian influenza, severe pneumonia, ARDS, and multiple organs dysfunction.

[Discussion]

In this case, the patient was radiologically demonstrated with diffuse small patches of dense opacity in both lungs that are ground glass like as well as integration of lesions and enlarged range with lesions along with progression of the condition.

For this case, the condition should be differentiated from highly pathogenic H5N1 avian influenza, seasonal influenza (including type A influenza H1N1), bacterial pneumonia, SARS, novel coronaviral pneumonia, adenoviral pneumonia, chlamydia pneumonia, and mycoplasma pneumonia. The definitive diagnosis is mainly based on etiological examinations.

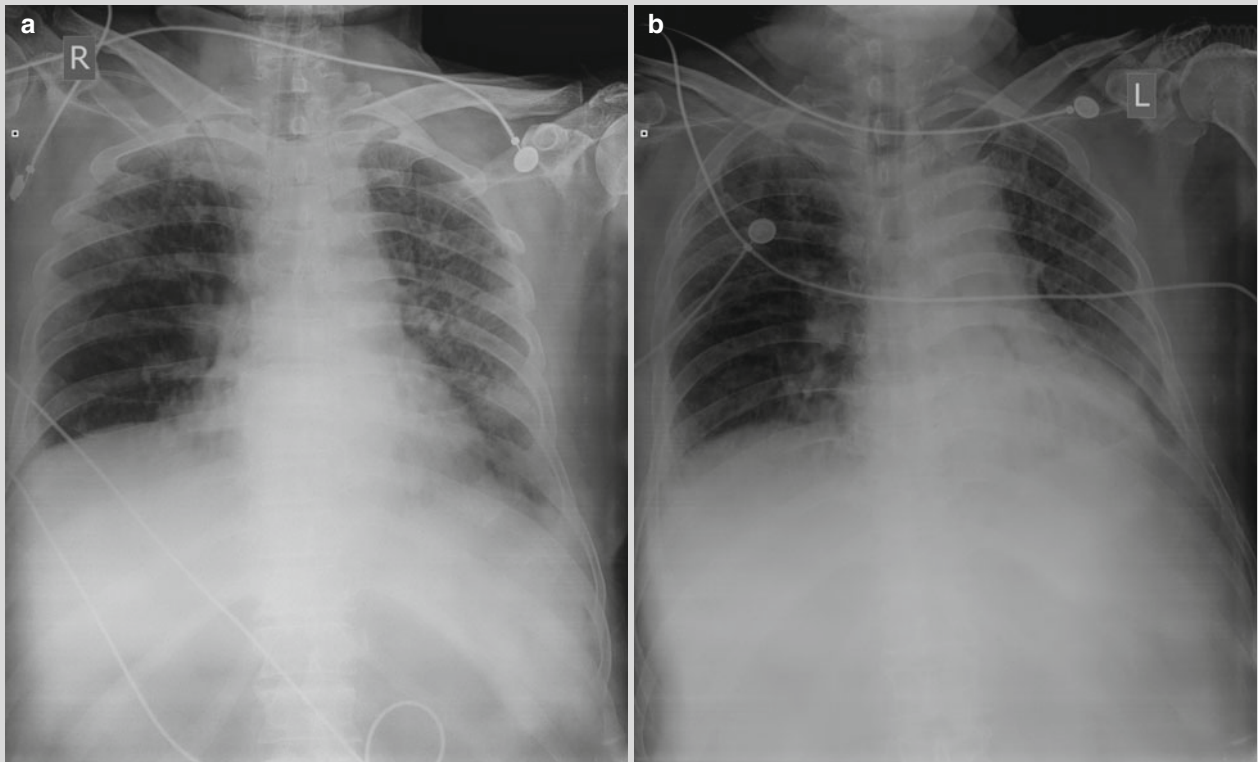


Fig. 11.2 Chest X-ray demonstrated diffuse small patches of dense opacity in both lungs that are ground glass like (a). Re-examination after 1 day showed diffuse small patches of dense opacity in both lungs that are ground glass like, with no obvious change compared to the previous chest X-ray (b). Re-examination after 3 days revealed diffuse small patches of dense opacity in both lungs that

are ground glass like, some of which are integrated; enlarged range with lesions in the left lung and the right upper lung; increased density of the opacity (c). Re-examination after 4 days demonstrated diffuse small patches of dense opacity in both lungs that are ground glass like, with further aggravation (d)

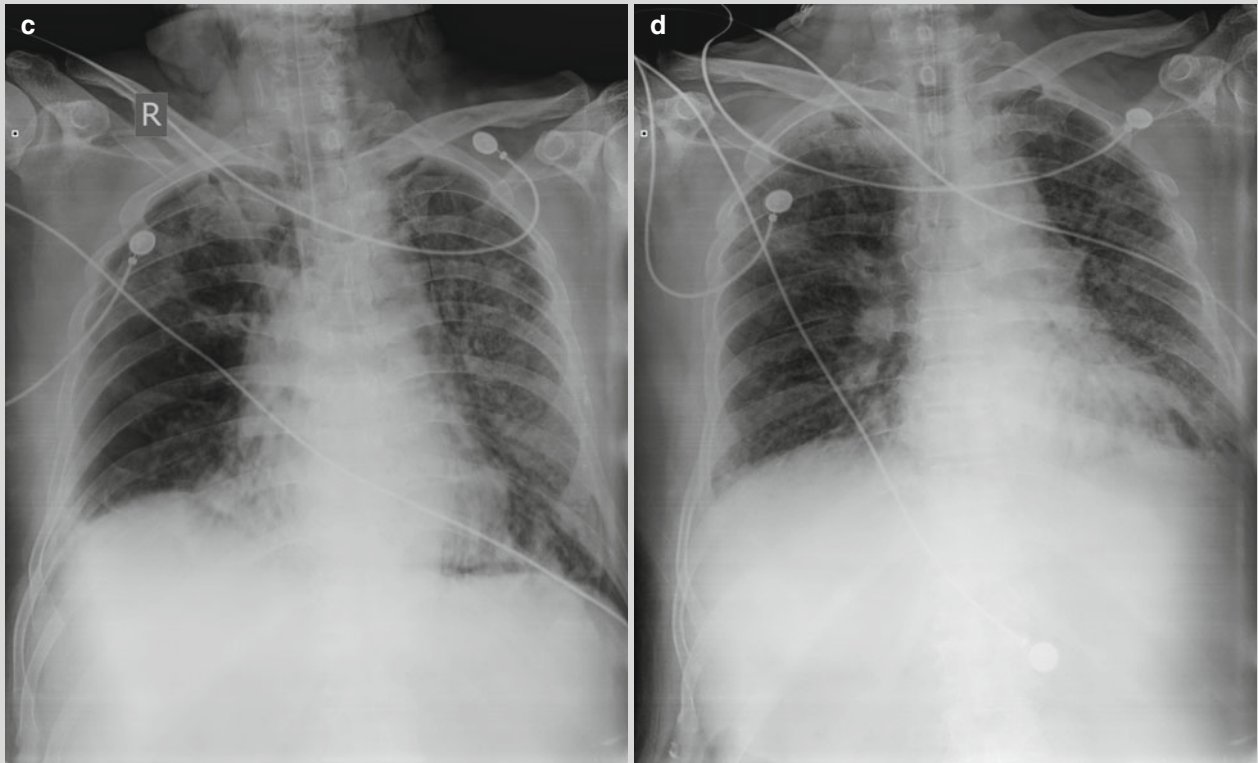


Fig. 11.2 (continued)

Case 3

[Brief Case History]

A 60-year-old man was hospitalized due to fever for 4 days and cough for 1 day. By physical examinations, his body temperature was 37.6 °C, with clear sound by lung percussion, clear breathing sounds by auscultation with no obvious dry and moist rales. Laboratory tests revealed WBC count $6.19 \times 10^9/L$, GR% 77.11%, MONO% 12.4%, lymphocytes ratio 10.32%, hs-CRP 85 mg/L, and ESR 9 mm/h. Serological test for *M. pneumoniae* was negative and blood biochemistry showed no abnormality. Chest CT indicated large high-density opacity with uneven density and poorly defined boundary in the lingual segment of left upper lung lobe. And the diagnosis was considered to be pneumonia of the left lung. After treatment for 2 days, the patient still experienced fever and was transferred into a large hospital for treatment. After that, the patient showed persistent fever with a body temperature of 37.6 °C. Bedside chest X-ray after 10 days demonstrated increased and blurry lung markings and multiple cotton like and flakes of opacity in both lungs. Bedside color Doppler ultrasonography showed liquid opacity in the right thoracic cavity and pericardium. And the patient experienced continuous decrease of oxygen saturation to around 60% and his blood pressure decreased

to around 70/50 mmHg. At that night, throat swabs by professionals from CDC showed positive and the diagnosis was defined to be human infection of H7N9 avian influenza virus. The patient was then transferred to the local hospital specialized in infectious diseases, and death occurred 1 week later. The patient reported a history of close contacts to feces of birds and chickens.

[Radiological demonstration] Fig. 11.3

[Diagnosis] Pneumonia induced by human infected H7N9 avian influenza.

[Discussion]

Human infected H7N9 avian influenza is a type A influenza, with the first 3 cases reported in Shanghai and Anhui province of China in Mar. 2013. Human infected H7N9 avian influenza virus is a newly emerging recombinant virus, which infects human via respiratory tract after contact to poultry with the infection. It has an incubation period of no more than 7 days. And the patients commonly experience flu like symptoms, such as fever, cough, expectoration of a little sputum as well as accompanying headache, muscle soreness and general malaise. In severe cases, the condition progresses rapidly into severe pneumonia, mostly with a body temperature of above 39 °C, dyspnea and possibly accompanying bloody sputum. Severe pneumonia may

further progresses rapidly into ARDS, mediastinal emphysema, sepsis, shock, consciousness disturbance, and acute renal damage. By chest radiology, the disease is characterized by primary lesions in one lung that gradually involve both lungs along with progression of the condition. In addition, the multiple lesions in both lungs show a multi-segmental and multi-lobar distribution. For this case, the patient had a history of close contacts to feces of birds, and the disease is radiologically characterized by inflammation of lobes in one lung at its early

stage. Along with the progression of the condition, both lungs are rapidly involved and ARDS finally occurred. The diagnosis was defined based on the finding of throat swabs to be a typical case of human infected H7N9 avian influenza. For this case, the condition should be differentiated from other types of pneumonia. Compared to other types of pneumonia, the patient in this case showed no obvious characteristic symptoms and physical signs and the definitive diagnosis is mainly based on the etiological examination.

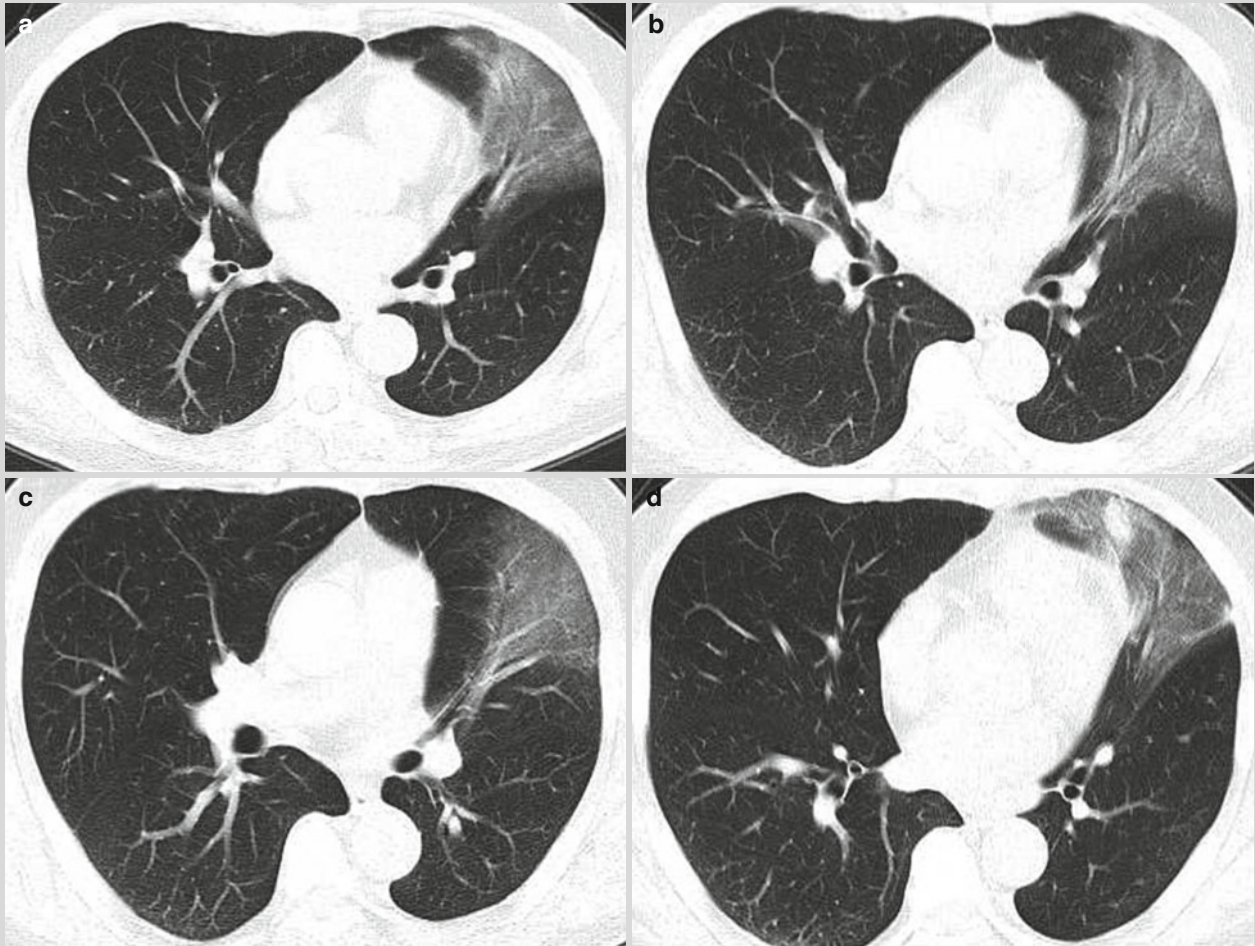


Fig. 11.3 CT scan demonstrated wedge shaped ground glass opacity in the lingual segment of left upper lung lobe, with high but uneven density, poorly defined boundary and air bronchogram inside (a–d)

Case 4**[Brief Case History]**

A 20-year-old woman complained of fever with the highest body temperature of 39 °C, headache, cough, expectoration of rust colored sputum, and systemic malaise for 1 day. Laboratory test showed WBC $3.8 \times 10^9/L$. She denied a history of contact to poultry.

[Radiological demonstration] Fig. 11.4

[Diagnosis] Severe pneumonia induced by human infected H7N9 avian influenza.

[Discussion]

For this case, the chest radiology demonstrated:

1. In the early stage, chest X-ray demonstrated ground glass opacity in one lung that showed lobar distribution with no opacity across the interlobar fissure.
2. The lesions were predominantly ground glass opacity that rapidly progressed to involve both lungs, with diffuse distribution and enlarged range with lesions. The GGO was shown to develop into consolidations with air bronchogram inside.
3. After positive treatment, the lesions were gradually absorbed and improved, with smaller range with lesions,

decreased density as well as evolvement into fibrous cords like, grid like and honeycomb like opacity.

Based on these radiological findings, we know that pneumonia induced by human infected H7N9 avian influenza resembles to other types of viral pneumonia, with concurrent parenchymal and interstitial involvements. However, pneumonia induced by human infected H7N9 avian influenza shows more obvious alveolar exudation in its early stage that overlaps lung interstitium. After partial absorption of alveolar exudation, fibrous cords like, grid like and honeycomb like opacity are radiologically demonstrated.

In this case, the condition should be differentiated from bacterial pneumonia and pneumonia induced by H1N1 influenza. By radiology, bacterial pneumonia is characterized by increased and blurry lung markings and nonspecific patchy opacity in both lungs, which is more common in bilateral middle and lower lung fields as well as middle and medial parts of both lungs. Clinically, WBC count increases. Pneumonia induced by H1N1 influenza shows early signs of GGO lesions in subpleural area and around bronchi. For this case, the differential diagnosis is challenging and should be based on virological detection.

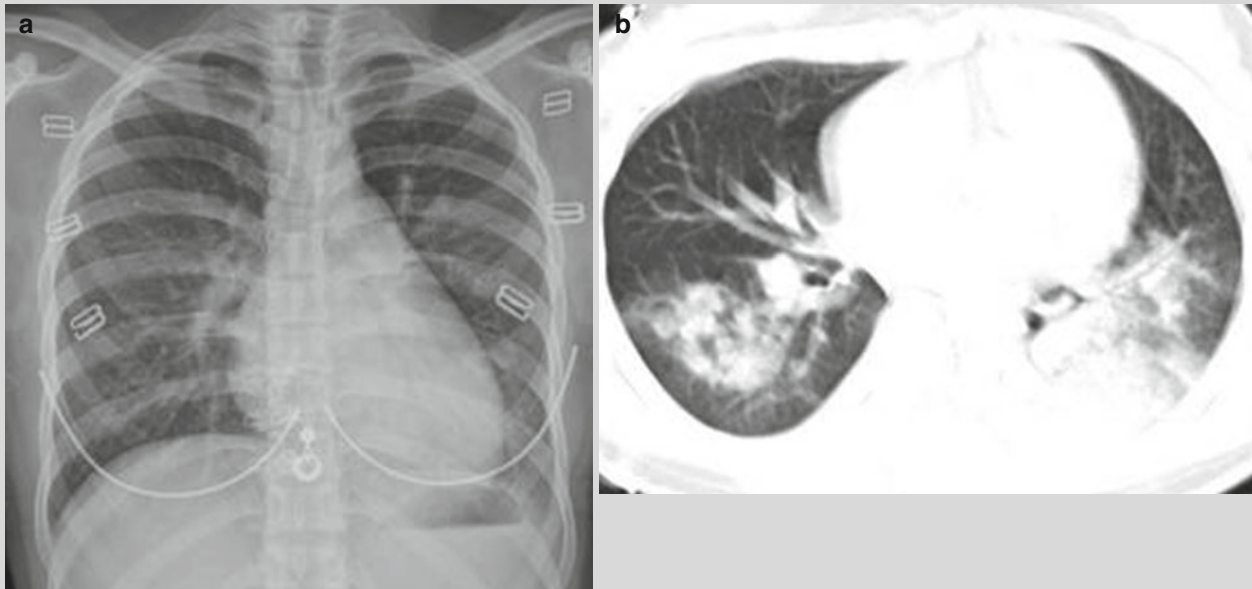


Fig. 11.4 Anterior-posterior chest x-ray 1 day after onset showed increased and thickened lung markings; small ground glass opacity in the left upper lung (a). Chest CT on d 3 after onset showed multiple patchy and nodular consolidations in both lungs, predominantly in the lower lung (b). Re-examination CT scan on d 5 after onset showed progression of the lesions into large consolidation, with air bronchogram inside (c). Re-examination after anti-viral

treatment on d 9 after onset showed obvious absorption of pulmonary lesions, with smaller range with lesions and decreased density (d). Re-examination by CT scan on d 12 showed further absorption of the lesions (e). Re-examination by CT scan on d 23 after onset showed fibrous cords like and honeycomb like opacity in both lungs (f)

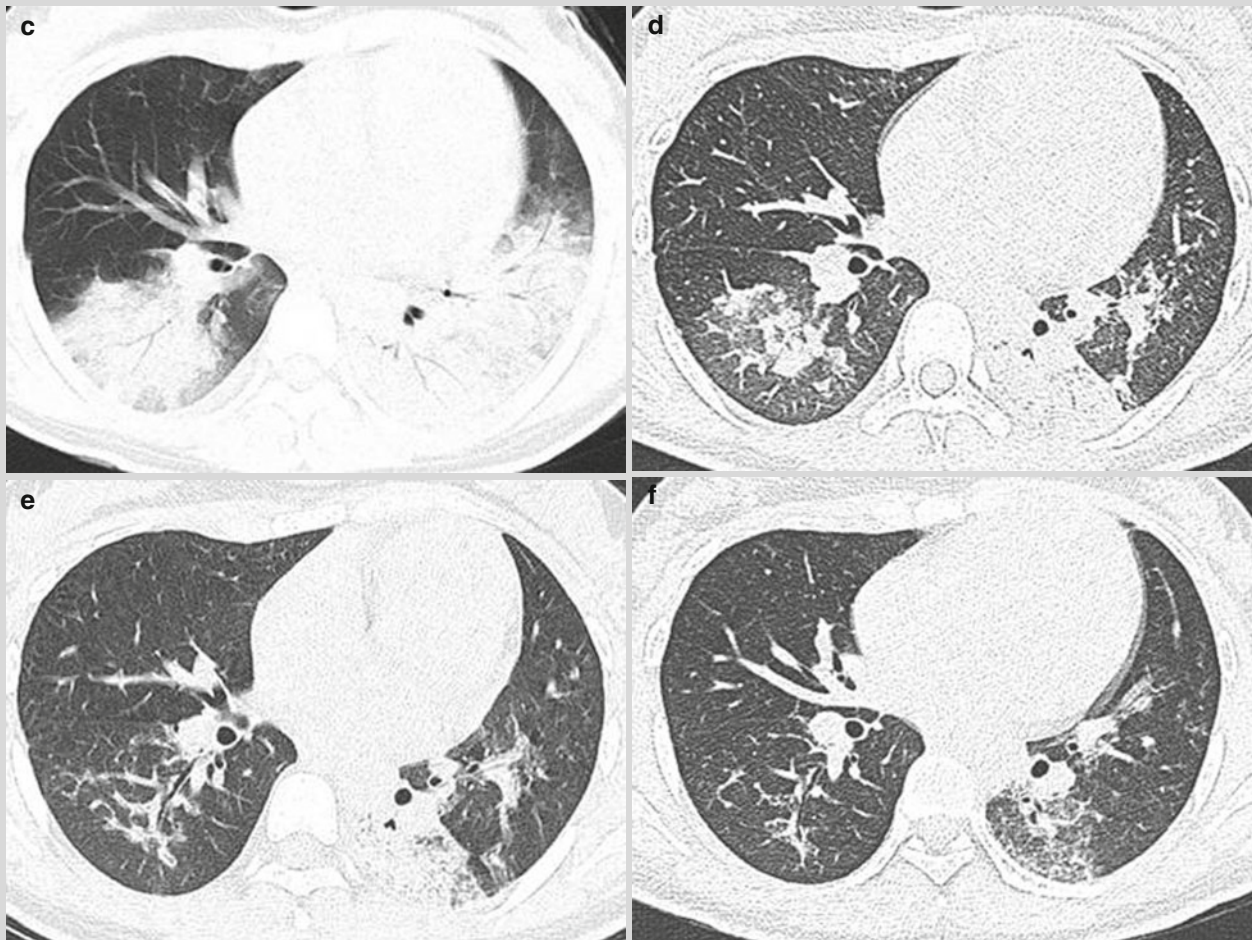


Fig. 11.4 (continued)

Case 5

[Brief Case History]

A 79-year-old woman experienced nasal obstruction, runny nose, fever with the highest body temperature of 39 °C, cough and expectoration. She denied a recent history of contact to poultry and denied a history of contact to patient with influenza. She was detected with nucleic acid of H7N9 avian influenza virus positive. Sputum culture revealed *A. baumannii* positive (++++), and aspergillosis positive. She had a medical history of cholestatic hepatocirrhosis as well as coronary heart disease and atrial fibrillation for 10 years. And she had medical history of right femoral neck fracture 4 months ago due to traumatic injury, which was treated by internal fixation and replacement. Currently, she was bedridden for a long period of time, and death finally occurred.

[Radiological demonstration] Fig. 11.5

[Diagnosis] Pneumonia induced by H7N9 avian influenza, Mixed lung infection by *Aspergillus* and *A. baumannii*.

[Discussion]

Recently, literature reports indicated that the susceptible populations to pneumonia induced by human infected H7N9 avian influenza include the elderly, those with underlying disease or compromised immunity. By CT scans, the most common sign is ground glass opacity, followed by consolidation, air bronchogram and interlobular septal thickening. The condition may be complicated by pleural effusion or air containing cyst. The lesions of the disease show a wide range, commonly involving 3 or more lung lobes. Qingle et al. reported a group of cases, with no formation of cavity. For this case, the patient was

an elderly, with medical histories of hepatocirrhosis, femoral neck fracture, long-term bedridden and compromised immunity. By sputum culture, *Aspergillus* was positive, indicating a complication of pulmonary aspergillosis, which is most likely the reason for intrapulmonary nodules and cavities. In addition, she also showed an infec-

tion of *A. baumannii* and death finally occurred. All the above clinical symptoms and radiological signs indicated that pneumonia induced by H7N9 avian influenza may be further complicated by fungal and bacterial infection, particularly in the elderly patients with poor condition of health and compromised immunity.

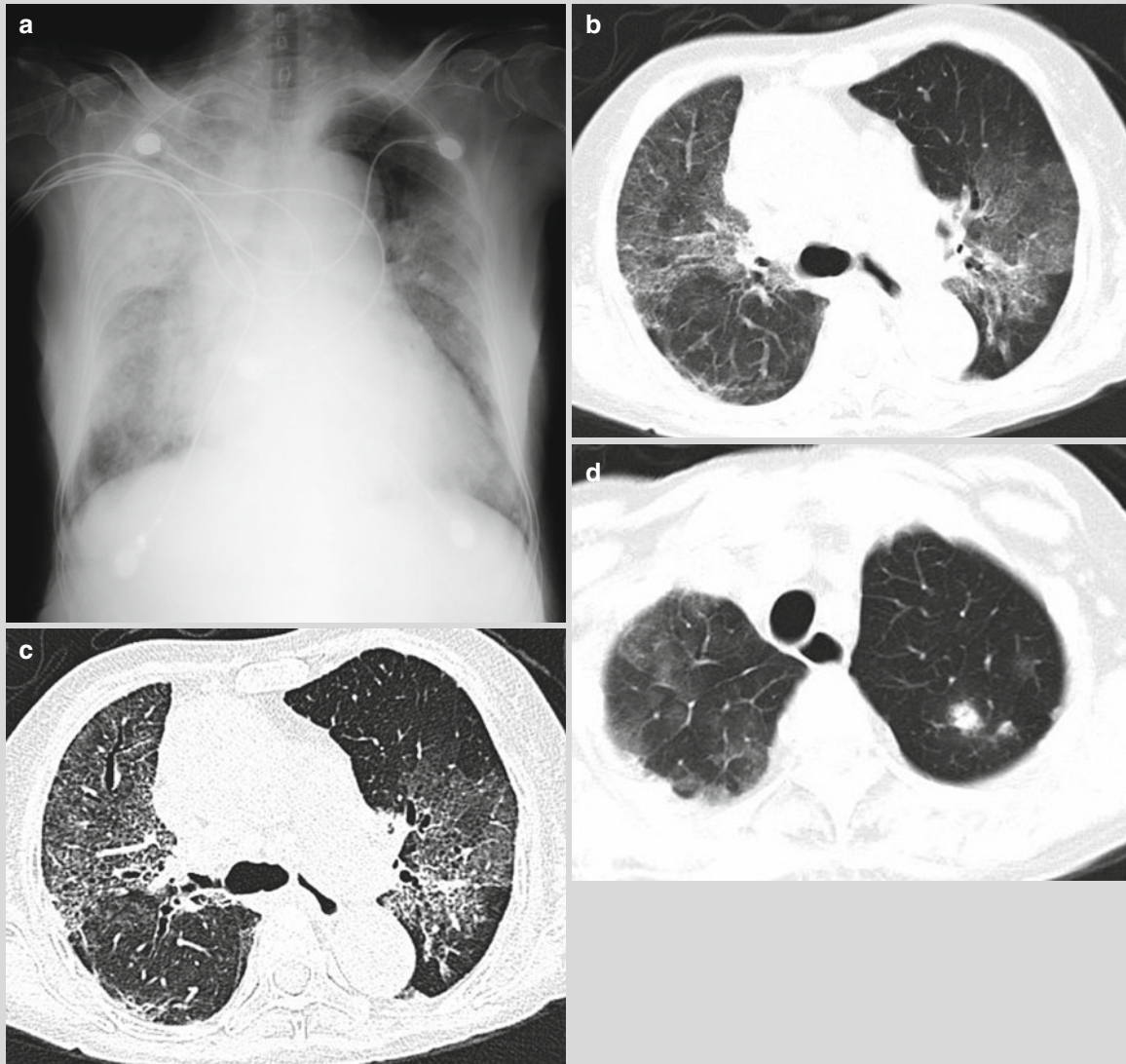


Fig. 11.5 Bedside chest X-ray demonstrated decreased transparency of both lungs, with diffuse large high density opacity that was more obvious in the right lung than in the left lung (a). CT scan showed diffuse ground glass opacity, grid like opacity, and flakes of high density opacity in both lungs; nodular opacity in the left upper lung lobe and in the right middle lung lobe; halo signs around the

nodules in the left upper lung lobe (c was the 1 mm reconstructed image of the same layer as b) (b–e). Re-examination by CT scan after 2 days showed no improvement of the lung lesions; cavity within the nodules in the left upper lung; halo sign around the nodules; obviously enlarged nodules in the right middle lung lobe (f, g)

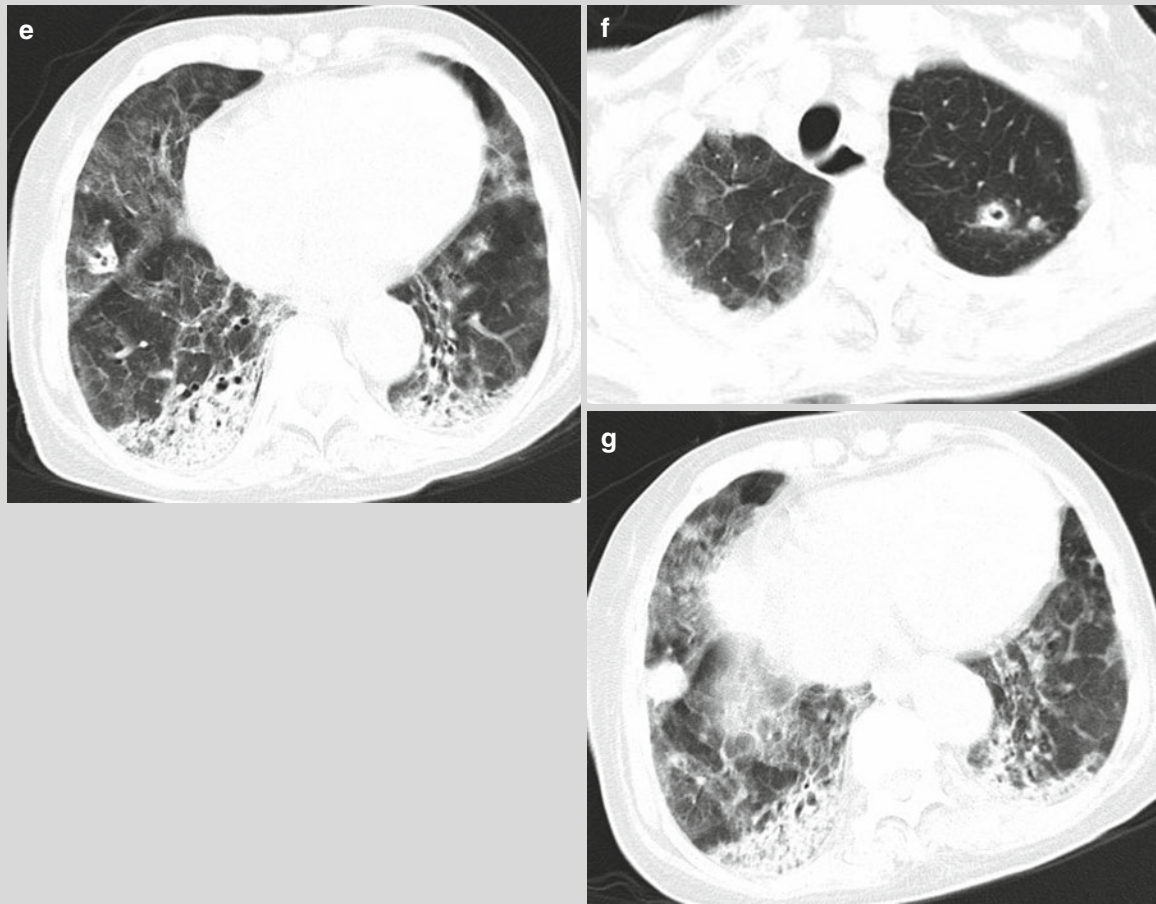


Fig. 11.5 (continued)

Case 6

[Brief Case History]

A 67-year-old man experienced fever, cough, and expectoration of a little whitish sputum, with the highest body temperature of 38.5 °C. He has no history of physical examination and other histories of underlying diseases. The nucleic acid test for H7N9 was positive.

[Radiological demonstration] Fig. 11.6

[Diagnosis] Pneumonia induced by human infected H7N9 avian influenza.

[Discussion]

The most common sign of pneumonia induced by human infected H7N9 avian influenza by CT scan is ground glass opacity, followed by consolidation, air bronchogram and interlobular septal thickening, possibly with pleural effusion. In some cases, air containing cyst can be observed, with a large area of involvement, commonly 3

or even more lung lobes. During the treatment, the condition may repeatedly improve and deteriorate, with the lung lesions firstly absorbed and then progress that is rapid in some cases. In some patients with good physical constitution and early diagnosis, the condition can be obviously improved after several days treatment, just like the present case. By CT scan, pneumonia induced by human infected H7N9 avian influenza is demonstrated with no specific signs, resembling to other viral pneumonia. And the final diagnosis should be based on clinical manifestations and laboratory tests. Radiological examinations play important role in guiding clinical treatment, monitoring disease progression, assessing therapeutic efficacy, and predicting the prognosis. Feng et al. scored the radiological demonstrations of pneumonia induced by human infected H7N9 avian influenza, which showed that a high score indicates a high mortality rate.

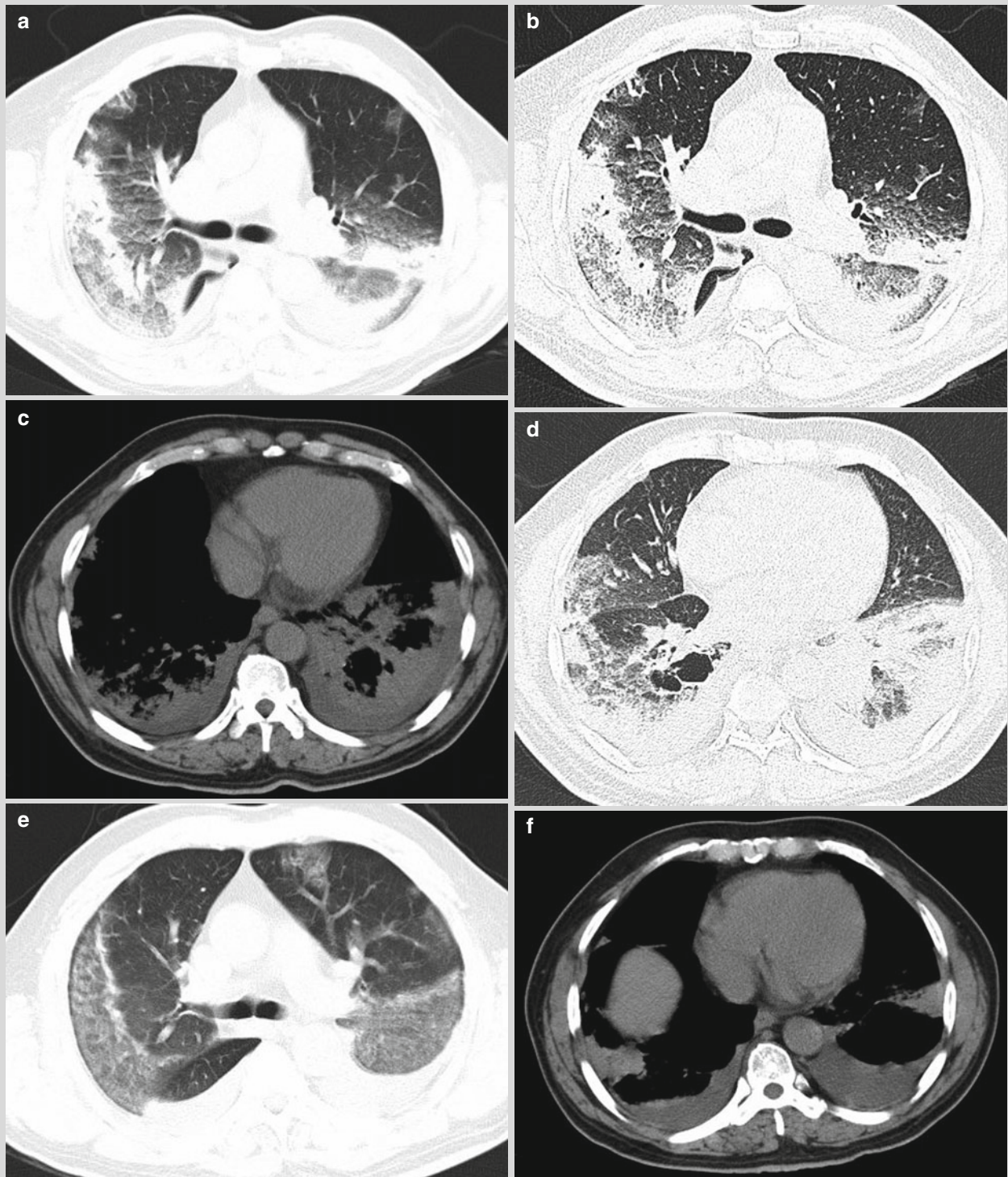


Fig. 11.6 CT scan showed multiple flakes of ground glass like and grid like high density opacities in both lungs, with air bronchogram within some lesions (**b** as the 1 mm reconstructed image of the same layer of **a**) (**a, b**). Bilateral pleural effusion in a small quantity (**c**). The basal segment of the right lower lung was shown with an irregular air containing cyst, with a little gas-fluid level (**d**). Reexamination after 4 days treatment, the lesions in the lungs were obviously absorbed (**e**). Bilateral pleural effusion progressed (**f**).

The air containing cyst in the right lower lung showed no obvious changes (**g**). Re-examination after 1 month, the lesions in lungs were obviously absorbed, still with flakes and grid like high density opacity that predominantly under the pleura (**i** as the 1 mm reconstructed image of the same layer of **h**) (**h, i**). Bilateral pleural effusion was completely absorbed. (**j**) The air containing cyst in the right lower lung was enlarged (**k**)

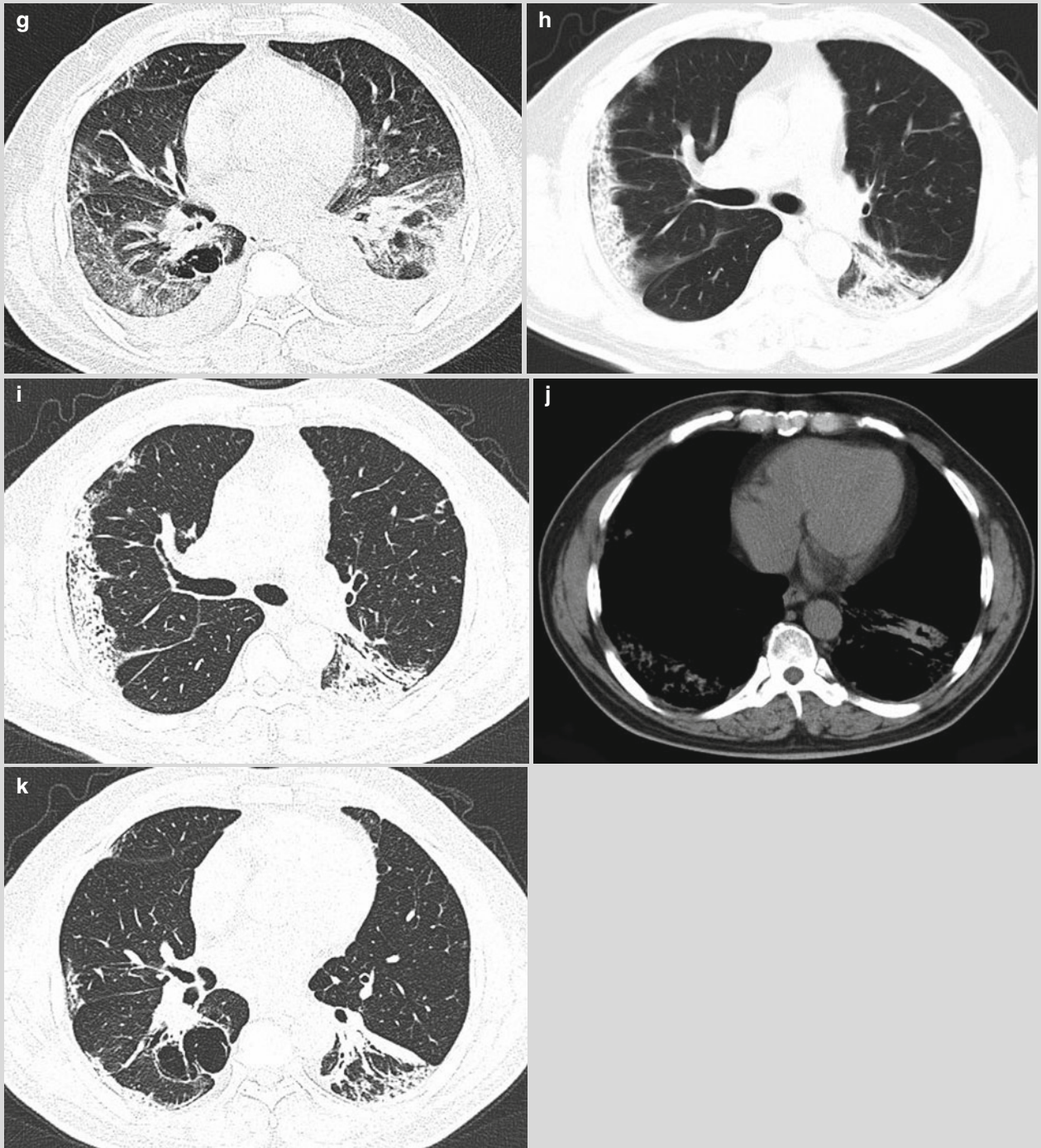


Fig. 11.6 (continued)

Case 7**[Brief Case History]**

A 33-year-old man, working as a cook, was hospitalized due to the chief complaints of chest distress for 5 days that deteriorated, with fever, cough and expectoration for 3 days. About 5 days ago, the patient caught a cold and began to experience chest distress that deteriorated after physical activities, and the body temperature within normal limits. About 3 days ago, his condition deteriorated, with inability of supine during nights, fever, cough, expectoration and a body temperature of 38.5 °C. By physical examination on admission, he was in a state of stupor, shortness of breath, heart rate 115/min, dullness by percussion of the right lung, coarse breathing sound of both lungs, dry rales of both lungs that predominantly right lung. Chest X-ray demonstrated multiple patches of opacity in both lungs that predominantly in the right lung. By laboratory tests, WBC $6.07 \times 10^9/L$, LY% 19.92%, CK 1431U/L, LDH 988U/L, CRP 58.8 mg/L, CD3⁺ CD8⁺ 36.6%, CD3⁻ CD56⁺ 15.9%.

Within 2–5 days after onset, the condition deteriorated rapidly, with occurrence of severe pneumonia and multiple organs dysfunction. In addition to the laboratory finding of H7N9 nucleic acid positive, he was diagnosed with human infected H7N9 avian influenza. After therapies of anti-viral therapy, anti-inflammatory therapy, the use of hormones and mechanical ventilation as well as symptomatic therapies for multiple organs dysfunction, his condition was obviously improved. Ten days after his hospitalization, tracheal intubation was removed, consecutive nucleic acid tests for 3 times showed negative, and the indexes for routine blood test, heart function, liver function and kidney function were within normal limits. He was then discharge after hospitalization for 28 days. Six months later, he began to experience superior tracheal stenosis, which was treated by tracheal stent implantation.

[Imaging manifestations] Fig. 11.7

[Diagnosis] Pneumonia induced by human infected H7N9 avian influenza.

[Discussion]

The diagnostic evidence for this case is as the following:

1. The patient reported a history of contact to secretions and excretions of poultry. And his condition developed rapidly, with the occurrence of severe pneumonia, multiple organs dysfunction, persistent increase of the body temperature since d 5 after onset. By laboratory tests, he showed no increase of WBC count but decrease of lymphocyte count, and H7N9 nucleic acid positive.
 2. By chest X-ray and CT scan, he showed multiple flakes of ground glass like and consolidation opacities in both lungs with air bronchogram. The lesions were in both lower lungs, predominantly the right lung, that progress rapidly and distribute extensively.
 3. After 10 days treatment by anti-viral therapy, use of hormones and mechanical ventilation, the lung lesions were absorbed and improved. Consecutive nucleic acid test for H7N9 for 3 times showed negative.
- Radiological evidence for the diagnosis is as the following:
1. The saliva acid of poultry, specifically binding to H7N9 avian influenza virus is mainly located in the lower respiratory tract, namely the lungs, but none in the upper respiratory tract. Human infection of H7N9 avian influenza virus directly induces pneumonia, with radiological signs of pneumonia early after onset.
 2. Early after onset, the lesions may be confined within one lung, the most commonly the right lung. If both lungs involved, the lesions distribute in multiple segments and multiple lung lobes that are predominantly and more serious in the right lung. In addition, the lesions in both lower lungs are more serious than in both upper lungs, which is possibly related to the posture for radiology and the anatomy of trachea. Radiologically, both the parenchymal and interstitial lesions are demonstrated as large consolidation, interlobular septal thickening, and sporadic ground glass opacity, with air bronchogram.
 3. During the progressive stage, human infected H7N9 avian influenza virus invades the lung tissues to induce the cytokine storm due to the absence of immunity to the new virus. Therefore, systematic inflammatory responses are triggered, with subsequent occurrence of acute respiratory distress syndrome (ARDS), shock and multiple organs failure. Radiologically, the lesions in lungs rapidly develop to involve multiple segments and lobes. Due to diffuse alveolar damages, chest X-ray and CT scan demonstrate extensively distributed ground glass opacity and consolidation opacity in both lungs, with air bronchogram, predominantly in both lower lungs or the right upper lung. In some cases, subpleural line and/or interlobular septal thickening is demonstrated; and in some other cases, pleural effusion. Pneumothorax and mediastinal lymphadenectasis may also be demonstrated.
 4. During the convalescent stage, the lung lesions are demonstrated with slow absorption, shrinkage, and lightening in color after active anti-viral therapy and

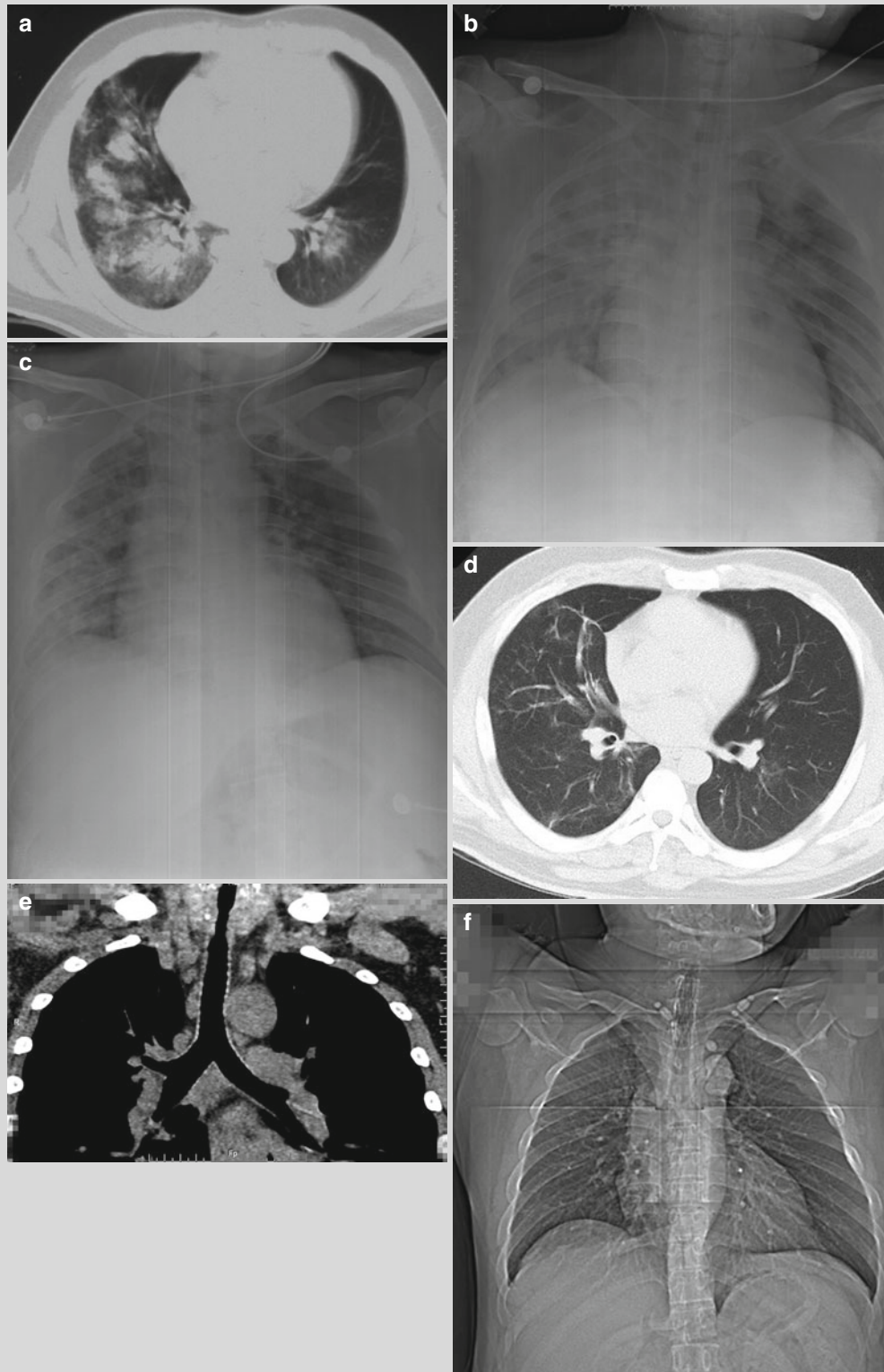


Fig. 11.7 On d 3 after onset, CT scan demonstrated nodular and flakes of consolidation opacity in the right lower lung, with air bronchogram inside; nodular consolidation in a small quantity in the left lower lung (a). On d 5 after onset, the lesions progressed rapidly. Chest X-ray showed multiple flakes of consolidation in both lungs that was predominantly in the right lung (b). On d 19 after onset, the respiratory symptoms were improved. Chest X-ray showed absorption and decrease of the consolidation (c). Reexamination 2 months

after onset, the patient was cured and discharged. CT scan showed fibrous cords like opacity in a small quantity in both lower lungs (d). Reexamination 6 months after onset, the patient began to experience chest distress again. Coronary reconstruction following tracheal CT scan showed superior tracheal stenosis, possibly related to tracheal intubation (e). Chest distress was immediately alleviated after tracheal stent implantation (f)

respiratory supportive therapy, with increased transparency of the lungs. The flakes of and nodular parenchymal lesions are rapidly absorbed, while the grid like and cords like interstitial lesions are absorbed slowly. Pleural thickening may persist for a long period of time. Due to the chronic stimulation by tracheal incubation, the symptoms of tracheal stenosis may occur.

Human infected H7N9 avian influenza should be differentiated from the following diseases.

1. Type A H1N1 influenza

Its early radiological signs include predominant GGO surrounding bronchovascular tree or in the subpleural area. And the lesions progress into extensive alveolar consolidation. Both pathologically and clinically, the changes are mild, with occurrence of death due to ARDS in rare critically ill patients. During the early stage of human infected H7N9 avian influenza, singular or multiple exudative lesions in multiple segments or lobes rapidly progress into ARDS and even multiple organs dysfunction. The diagnosis can be defined based on nucleic acid test of the virus.

2. Sever acute respiratory syndrome (SARS)

Radiologically, both lungs are demonstrated with diffuse GGO and extensive consolidation. The lesions progress rapidly, mostly distribute in the lungs periphery and mainly involve the subpleural area. The interstitial lesions of SARS are more obvious than those of human infected H7N9 avian influenza, with interlobular septal thickening in paving-stones sign by HRCT.

3. Bacterial infection

In the cases of lobar pneumonia, both WBC and neutrophil counts show significant increase. The lesions commonly involve one lung, more commonly the right lung, and multiple lobes involvement is rare. During its consolidation period, the lesions are commonly dense with air bronchogram. However, human infected H7N9 avian influenza is characterized by WBC count within normal limits and decreased lymphocyte count. The lesions rapidly develop into consolidations in multiple segments and lobes as well as ARDS. Thoracic bacterial infection may occur during treatment due to poor immunity of the patient, tracheal intubation and the use of hormones in a large quantity.

Case 8

[Brief Case History]

A 56-year-old man complained of fever (with the highest body temperature of 39.5 °C), sore throat and muscle soreness for 6 days with no known causes. His condition was hardly improved after anti-viral and symptomatic therapies, with occurrence of cough and expectoration for 2 days as well as chest distress, shortness of breath and consciousness disturbance for 1 day. Arterial blood gas analysis indicated respiratory acidosis and carbon dioxide retention. He reported no history of contact to poultry but a medical history of thymoma and its surgical removal.

[Radiological demonstration] Fig. 11.8

[Diagnosis] Pneumonia induced by human infected H7N9 avian influenza; severe pneumonia; type II respiration failure.

[Discussion]

After onset of clinical symptoms, the patient was diagnosed with ordinary influenza and corresponding therapy was given, with no obvious therapeutic efficacy. He paid no attention to his condition until its deterioration and received anti-viral therapy and respiratory supportive therapy. The initial radiological examination showed lobar and

segmental consolidation of one lung, which resembles to those in the consolidation period of lobar pneumonia. After 6 days, the pulmonary lesions obviously progressed and were diffusely distributed in both lungs. In the following radiological examinations, the lesions deteriorated again, with gradual deterioration following slight absorption of the lesions and subsequent slow absorption. Based on clinical manifestations and laboratory tests, it was speculated that it may be related to occurrence of mixed infection in the late stage of the disease. Long-term following up observation indicated that the lesions are subject to interstitial fibrosis after their absorption.

In this case, differential diagnosis should be made from lobar pneumonia during its early stage. But it is challenging because both diseases show extremely similar radiological signs. However, in the patients with lobar pneumonia, clinical symptoms and signs can be obviously improved after administration of antibiotics and symptomatic therapy. But in this case, active therapies showed no obvious therapeutic efficacy, and the condition of the patient aggravated. Such outcomes should be paid focused attention and its etiological evidence should be traced to change therapeutic regime.

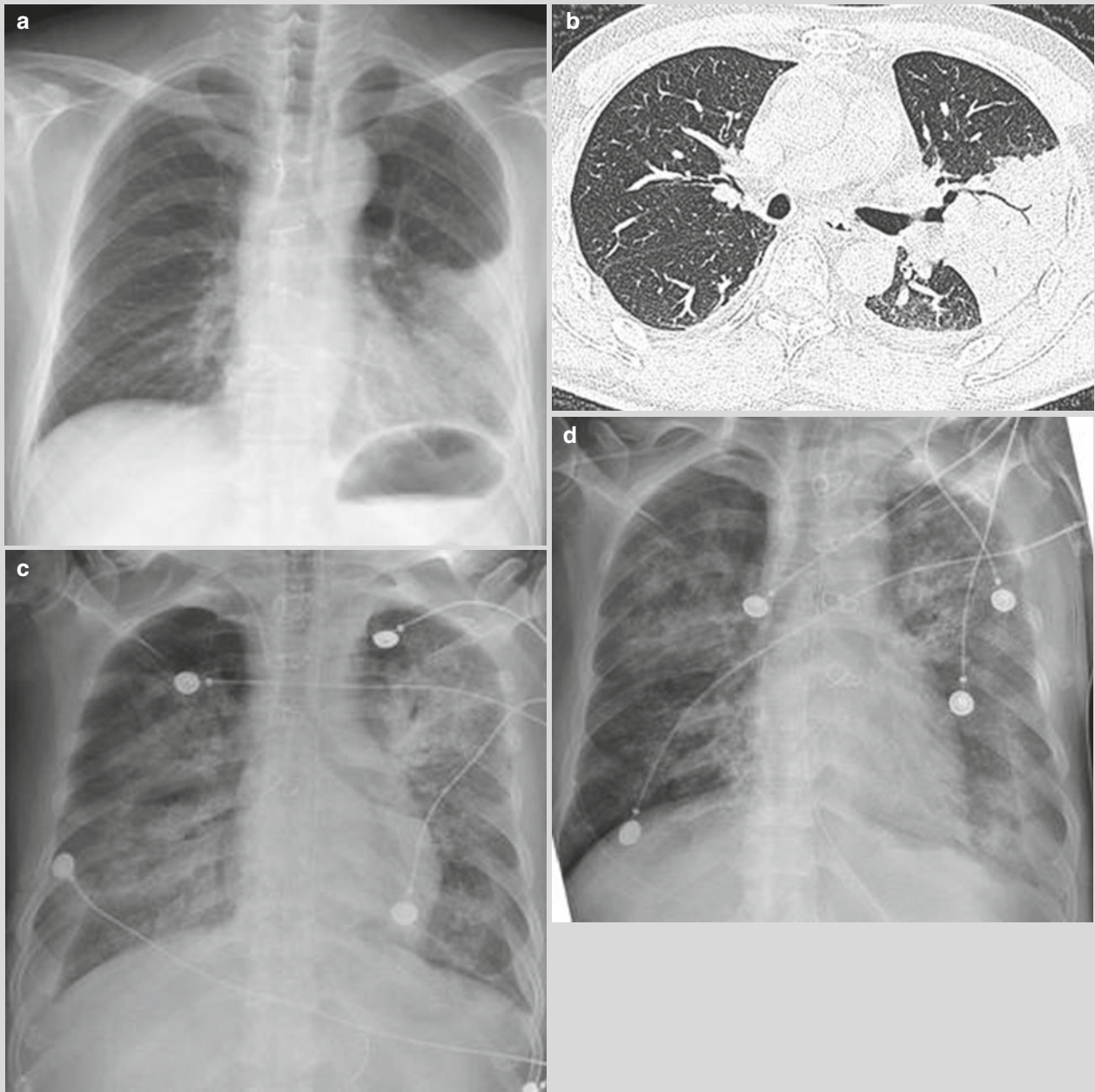


Fig. 11.8 On d 7 after onset, anterior-posterior chest X-ray demonstrated lobar segmental consolidation in the left lower lung field (a). CT scan showed consolidation in the left upper lung lobe, with air bronchogram inside (b). On d 13 after onset, bedside chest X-ray showed diffuse flakes of consolidation and ground glass opacity in both lungs (c). On d 18 after onset, bedside chest X-ray showed absorption of the lesions in the right lower lung but aggravating lesions in the left lower lung (d). On d 28 after onset, CT scan showed large consolidation in both lungs and aggravated consolida-

tion in the right lower lung, with interlobular septal thickening (e). On d 31 after onset, bedside chest X-ray demonstrated absorption of the lesions in the left lung in grid like and honeycomb like changes (f). On d 32 after onset, CT scan showed interstitial thickening predominantly in the left upper lung, slightly decreased density of consolidation in the left lower lung, and obvious consolidation in the right lung (g). By reexamination 18 months after the onset, CT scan showed a small quantity of residual fibrous cords like opacity, indicating fibrosis (h)

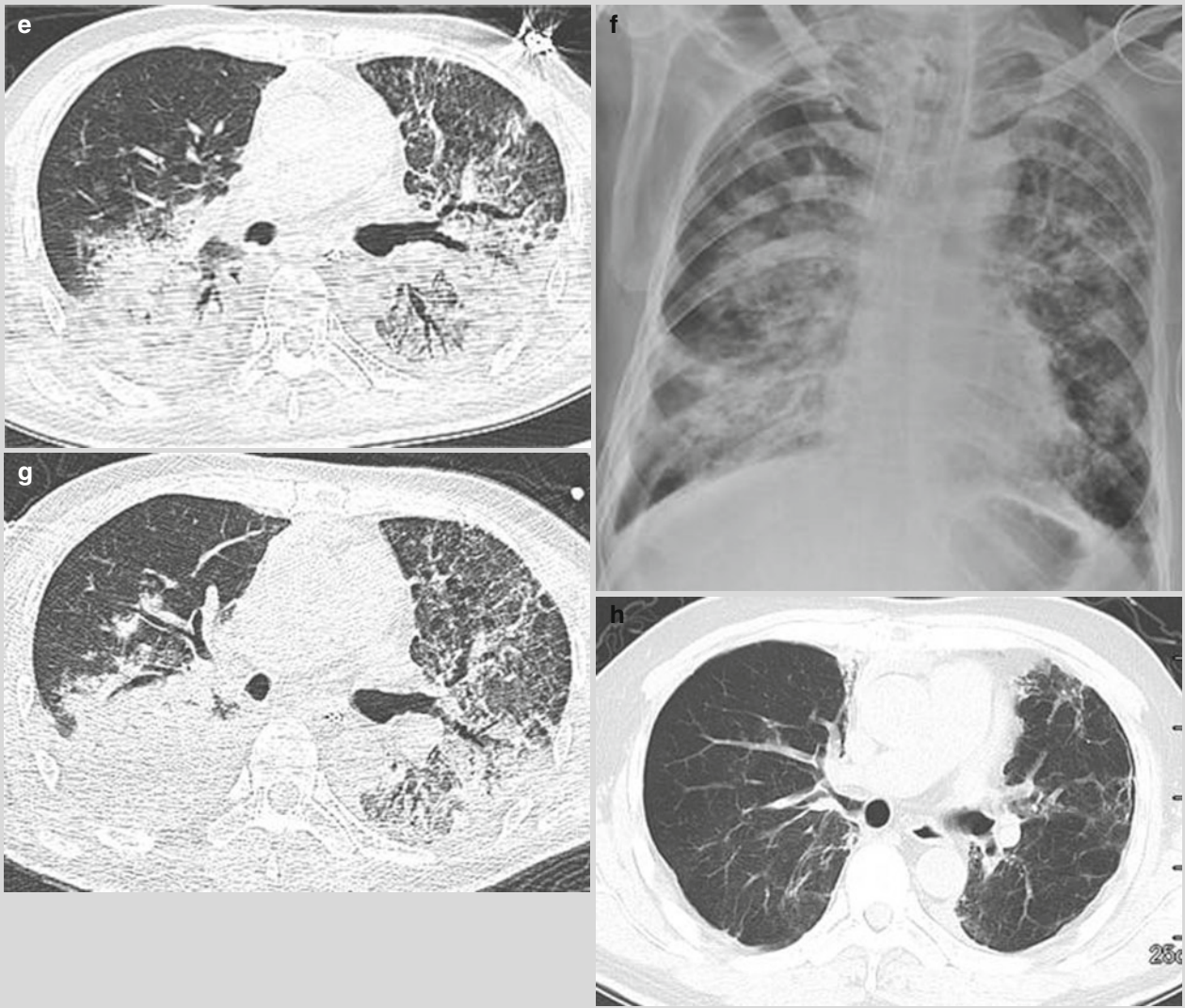


Fig. 11.8 (continued)

Case 9

[Brief Case History]

A 38-year-old man complained of fever with no known causes with the highest body temperature of 39.4 °C since Dec. 9, 2013, accompanying paroxysmal cough and expectoration of yellowish white thick sputum in a small quantity. He paid a clinic visit in a local hospital. But on Dec. 12, 2013, he was hospitalized due to aggravation of the condition. Chest X-ray showed large consolidation in the left lower lung and sporadic patches of opacity in the right lung. One day after treatment, these symptoms aggravated. Blood gas analysis showed type I respiratory failure. After that, the patient was transferred into ICU. By physical examination on admission, his body temperature 36.1 °C, heart rate 116/min, breathing rate 36/min, and blood pressure 116/67 mmHg. He respired with the assistance of ventilators and showed no response to calling. Conjunctiva slightly swollen in both eyes, with no congestion, no yellowish sclera, equal size of bilateral pupils in a diameter of about 2 mm that are sensitive to light. Pharynx congested, bilateral tonsils no swelling, no special abnormality in heart examination. Fremitus weakened at the left chest, no sensation of pleural friction; dullness of the left lower lung by percussion; coarse breathing sounds of both lungs that was relatively weaker in the left lung; fine moist rales in both lungs. He reported a history of buying chicken in a market and cooking it on Nov. 20, 2013. Routine blood test showed WBC $3.48 \times 10^9/L$, GR% 76.1%. Blood biochemistry revealed CK 3319U/L, LDH 882U/L, CKMB 32.5U/L, K^+ 2.83 mmol/L, Na^+ 133 nmol/L, troponin and BNP within normal limits, CRP 26.71 mg/L, ALT 136U/L, AST 470U/L, ALB 27 g/L. Blood gas analysis showed pH 7.48, PO_2 47 mmHg, PCO_2 25.4 mmHg, and BE -5 mmol/L. CD4 T cell count was 42/ μ l. By etiological examination, his tracheal aspirates showed H7N9 nucleic acid positive.

[Radiological demonstration] Fig. 11.9

[Diagnosis] Pneumonia induced by human infected H7N9 avian influenza.

[Discussion]

For this case, the symptoms and signs are in line with the diagnostic criteria of severe pneumonia induced by human infected H7N9 avian influenza established by the National Health and Family Planning Commission of

China. At the early stage, the patient showed pulmonary consolidation, with complication of pleural effusion. And radiologically, the lesions are characterized by the following:

1. On d 3 after onset, plain chest X-ray showed poorly defined patches of opacity in the left middle and lower lung fields as well as left pleural effusion; ground glass opacity in the right middle lung field. Chest CT scan on the same day demonstrated patches of ground glass opacity in the right middle lung lobe and the left upper lung; large consolidation in the left lower lung lobe, with air bronchogram inside.
2. On d 14 after onset, the lesion of lung consolidation was obviously absorbed, with patches of GGO in the right upper and middle lung and the left upper lung, predominantly in the subpleural areas; the lesion of consolidation in the left lower lung was absorbed compared to previous CT scan findings. And the air opacity in the anterior mediastinum and the anterior thoracic wall is induced by invasive ventilation.
3. Reexamination by chest CT scan on d 39 after onset revealed almost absorbed GGO in both lungs and consolidation in the left lower lung; but observable lesions of pulmonary interstitial fibrosis, such as small GGO in lower lungs and interlobular septal thickening. In addition, the gas opacity in the anterior mediastinum and anterior thoracic wall was also absorbed.

Pneumonia induced by H7N9 avian influenza should be differentiated from other emerging infectious diseases, such as viral pneumonia induced by H5N1 avian influenza virus and type A H1N1 influenza virus as well as SARS. Radiologically, they share commonalities of GGO and consolidation, with rapid change and progression. Early lesions of pneumonia induced by H7N9 avian influenza are predominantly located in both lower lungs, which is not characteristic of pneumonia induced by H5N1 avian influenza virus or type A H1N1 influenza virus and SARS. Therefore, its differential diagnosis based on radiology is challenging, and clinical diagnosis should be defined based on epidemiological investigation and etiological examination.

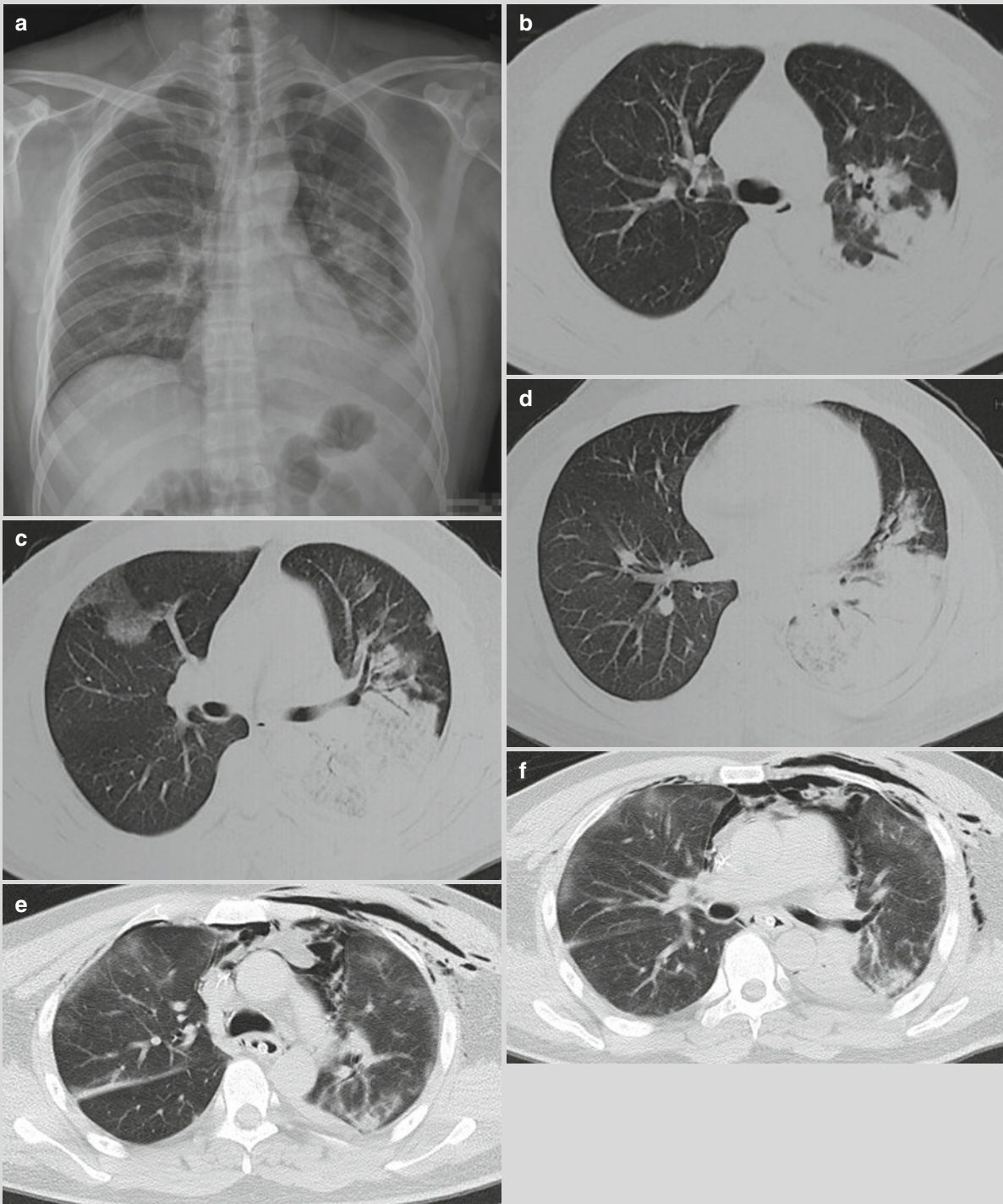


Fig. 11.9 On d 3 after onset, chest X-ray showed large flakes of high density opacity in the left middle and lower lung fields, with poorly defined boundary; flakes of ground glass opacity in the right middle lung field; and blunt left costophrenic angle (a). On d 3, chest CT scan showed irregular flakes of opacity in the apical posterior segment of left upper lung lobe (b). Patches of ground glass opacity in the right middle lung lobe and the left upper lung lobe; large consolidation in the left lower lung lobe (c). Shrinkage of the left lower lung lobe was shown, with large consolidation and air bronchogram inside (d). On d 14, chest CT scan demonstrated flakes of ground glass opacity in both upper lungs; gas opacity in the anterior mediastinum and the thoracic wall (e).

Ground glass opacity was observable under the pleura in the right middle lung lobe and the left upper lung; flakes of consolidation adjacent to the chest aorta in the left lower lung lobe; gas opacity in the anterior mediastinum and the thoracic wall (f). Pleural effusion in a small quantity was detected in the right pleural cavity; large consolidation in the left lower lung with air bronchogram inside; gas opacity in the anterior mediastinum and the left anterior thoracic wall (g). On d 39, chest CT scan demonstrated interlobular septal thickening in the dorsal segment of the left lower lung lobe, with local pleural thickening (h). Flakes of ground glass opacity was observed in the dorsal segment of left lower lung lobe, predominantly in the left lower lung lobe (i)

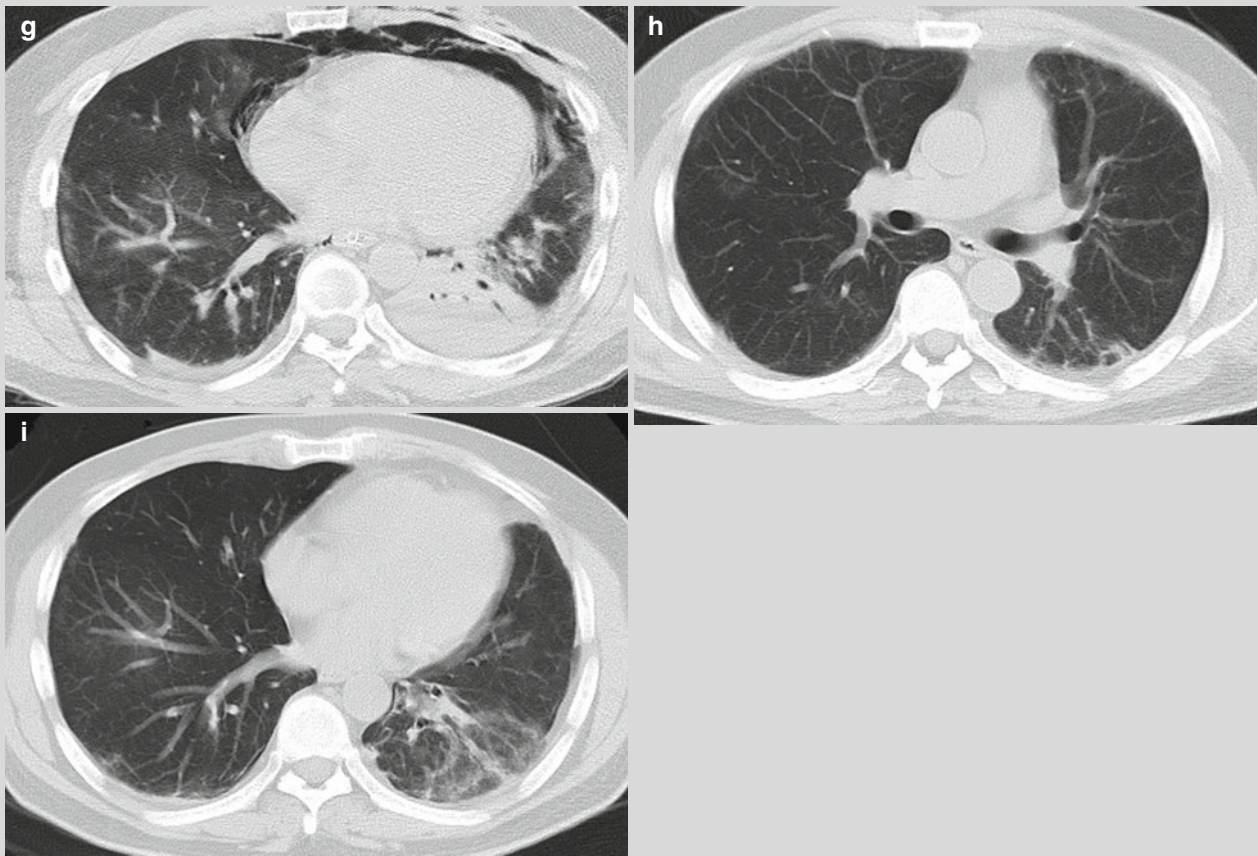


Fig. 11.9 (continued)

Case 10

[Brief Case History]

A 55-year-old man experienced frequent paroxysmal cough and expectoration of a little yellowish white thick sputum since Jan. 5, 2014. His condition was diagnosed as hypertension due to a blood pressure of 154/96 mmHg and he received medication to lower his blood pressure. Several days later, he was hospitalized on Jan. 10, 2014 due to the aggravating condition. Chest X-ray revealed bronchiectasis in the left lower lung with accompanying infection, which was then considered as lung infection. He was then admitted to the Respiratory Department for treatment, but his cough was not improved by anti-infection therapy. On Jan. 13, 2014, he still experienced fever, with the highest body temperature of 38 °C. An immediate blood gas analysis indicated respiratory failure, and he was transferred to ICU for tracheal intubation and assisted breathing via ventilator. Bedside chest X-ray revealed extensive infection in both lungs and possible bronchiectasis in left lower lung, indicating significant progression compared to the condition on

Jan. 10, 2014. Routine blood test showed WBC count $2.61 \times 10^9/L$, GR% 70.9%, RBC count $5.0 \times 10^{12}/L$, HGB 158 g/L, PLT $71 \times 10^9/L$. Blood gas analysis revealed pH 7.45, PO₂ 50 mmHg, and PCO₂ 24 mmHg. On Jan. 13, 2014, laboratory test by CDC showed reported alveolar lavage fluid positive to H7N9 avian influenza virus, and peripheral CD4 T cell count 66/μl.

[Radiological demonstration] Fig. 11.10

[Diagnosis] Pneumonia induced by human infected H7N9 avian influenza.

[Discussion]

In this case, the patient was an elderly man with no definitive history of contact to live poultry. The onset symptoms include cough and expectoration, and laboratory tests showed decreased peripheral WBC count, decreased platelet count, and decreased blood potassium level. On d 5 after onset, chest X-ray revealed infection in the left lower lung. The patient experienced repeated fever and the condition rapidly progressed into respiratory failure, multiple organs failure and infectious shock.

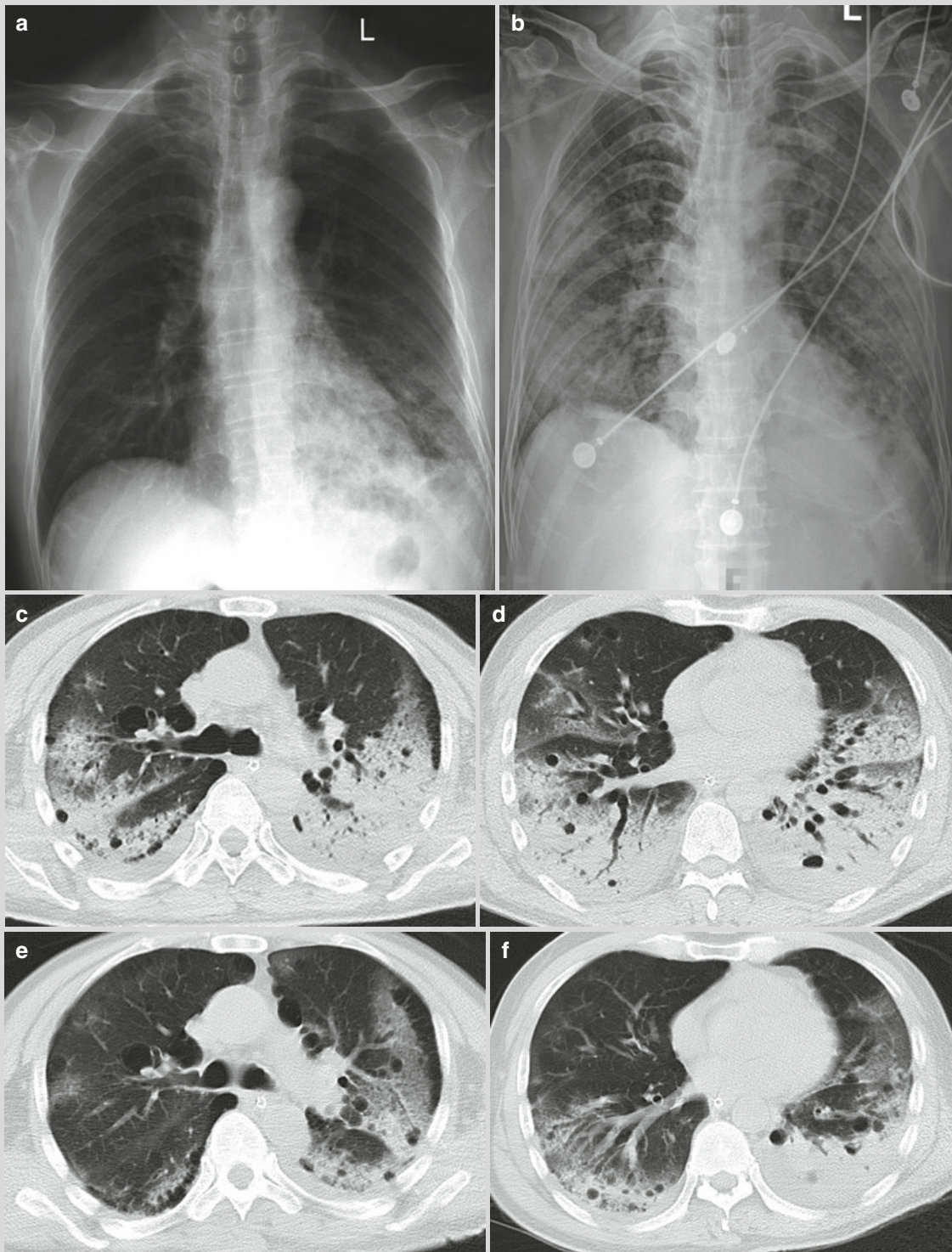


Fig. 11.10 On d 5 after onset, chest X-ray showed poorly defined patches of high density opacity in the left lower lung field; overlapping of some lesions with heart shadow (a). On d 8 after onset, chest X-ray showed flakes of ground glass opacity in both lungs, and consolidation in the bilateral middle and lower lung fields (b). On d 9 after onset, chest CT scan showed multiple large high density opacity and ground glass opacity in both lower lung lobes, predominantly in the left lower lung lobe (c). Large consolidation was revealed in both lower lungs, with air bronchogram and multiple cystic translucent areas (d). On d 14, chest CT scan showed unevenly distributed ground glass opacity in the bilateral upper and middle lung lobes,

consolidation in the left upper lung with multiple small translucent areas with no wall (e). Both lower lungs were revealed with patches of GGO like high density opacity and the left lower lung was shown with large consolidation and round translucent opacity in different sizes inside. They were mainly distributed in the left subpleural area and the dorsal lungs. Compared to the chest CT scan film 5 days ago, the lesions were absorbed (f). On d 209, the left lung was shown with unevenly distributed ground glass opacity; the left subpleural area and anterior mediastinum were shown with lung bullae (h). Lung bullae were sporadic in both lower lung lobes (h)

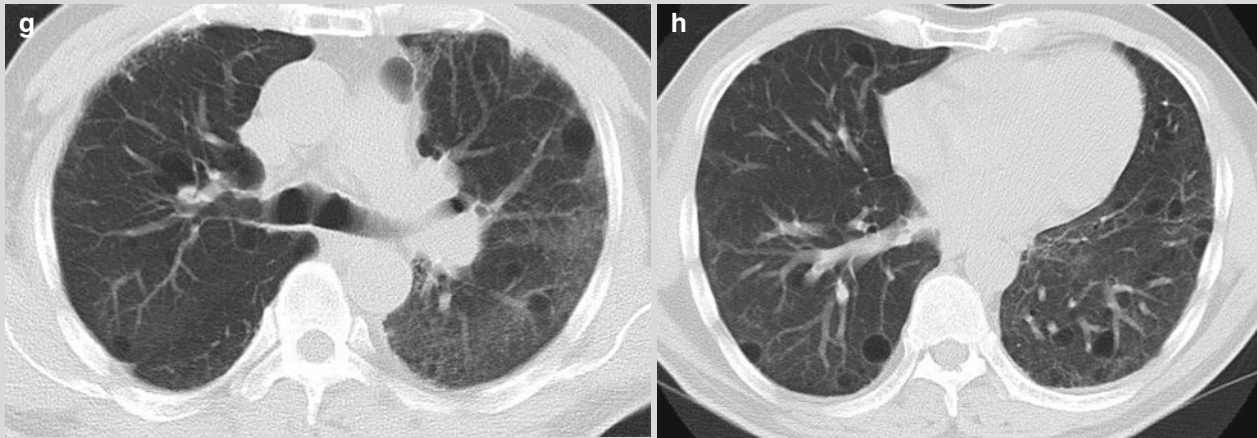


Fig.11.10 (continued)

On d 5 after onset, chest X-ray indicated infection in the left lower lung and on d 8 after onset, the lesions spread to involve both lungs. On d 9 after onset, chest CT scan revealed large consolidation and ground glass opacity in each lobe of both lungs, with multiple small translucent areas inside. These radiological signs indicated rapid progression of the lesions, which are rarely observed in patients with bacterial and common viral pneumonia.

This case is radiologically characterized by the followings:

1. The lung lesions are mainly consolidation and GGO, which emerge early after onset. And the lesions are

mainly distributed in the subpleural area of both lower lung lobes. Air bronchogram is observable in the consolidation opacity.

2. The lesions progress rapidly but are absorbed slowly. The lesions are firstly confined within one lung, but rapidly spread to involve lobes and segments of both lungs. The condition rapidly develops into respiratory failure. With the use of various therapies, the lung lesions are gradually absorbed, with slower absorption of interstitial lesions than parenchymal lesions.

Case 11**[Brief Case History]**

A 39-year-old woman experienced cough and expectoration of yellowish sputum with no known causes since Jan. 15, 2014. Her condition was not improved after treatment in a local hospital on Jan. 17. And she was then hospitalized in a superior hospital due to a diagnosis of lung infection. Physical examinations showed a body temperature of 38 °C, heart rate 95/min, respiration rate 19/min and blood pressure 123/73 mmHg. She was well conscious in good spirits, no shortness of breath, and cooperative to the physical examinations. By palpation, the swallow lymph nodes no enlarged, and 3 depression sign negative (-). Pharynx congested, bilateral tonsils no swollen with no pus spots, and oral cavity no Koplik's spot. The chest no malformation, bilateral breathing mobility equal, breathing sounds of both lung coarse, moist rales in the right lower lung, and no pleural friction sounds. The heart beat rhythm regular, and no murmurs by auscultation. The abdomen was soft, liver and spleen unpalpable under ribs, the whole abdomen no tenderness and rebound, and bowel sound normal. Both lower limbs no swollen. She denied medical histories of other diseases but experienced vomiting, nausea and pruritus of right lower leg after oral intake of Cephaloridine 1 day ago. She also denied a history of contact to live poultry, but reported a history of eating chickens 6 days ago. Routine blood test showed WBC count $5.2 \times 10^9/L$, GR% 63%, and LY% 30.1%. Blood gas analysis revealed pH 7.47, PCO_2 31 mmHg, PO_2 67 mmHg, Na^+ 134 mmol/L, K^+ 2.7 mmol/L, and Ca^{2+} 0.91 mmol/L. Sputum test showed nucleic acid of H7N9 avian influenza virus positive.

[Radiological demonstration] Fig. 11.11

[Diagnosis] Pneumonia induced by H7N9 avian influenza.

[Discussion]

This case is radiologically characterized by the followings:

1. On d 2 after onset, chest plain X-ray showed small flake of high density opacity at the cardiophrenic angle of right lower lung field, indicating emergence of lesions in lower lung in the early stage of pneumonia induced by human infected H7N9 avian influenza. On d 3 after onset, chest X-ray further proved flake of GGO in the posterior basilar segment of right lower lung lobe, and opacity with mixed GGO density with parenchymal density.
2. On d 6 after onset, chest CT scan demonstrated rapid progression of the lesions in both lungs, with large consolidation in the right lower lung lobe and sporadic poorly defined patches of opacity in the right middle lung lobe and each basilar segment of the left lower lung lobe. Within 72 h, the progression of lesions was more than 50%, which was in line with the diagnostic criteria of severe pneumonia induced by human infected H7N9 avian influenza.
3. At the peak of lesion progression, the lesions began to be absorbed after effective therapy was given, but the convalescent stage lasted for a relatively long period of time. On d 31 after onset, chest CT scan showed absorption of most lesions but still residual cords like opacity and small GGO in the subpleural area of posterior basilar segment in the right lower lung lobe.

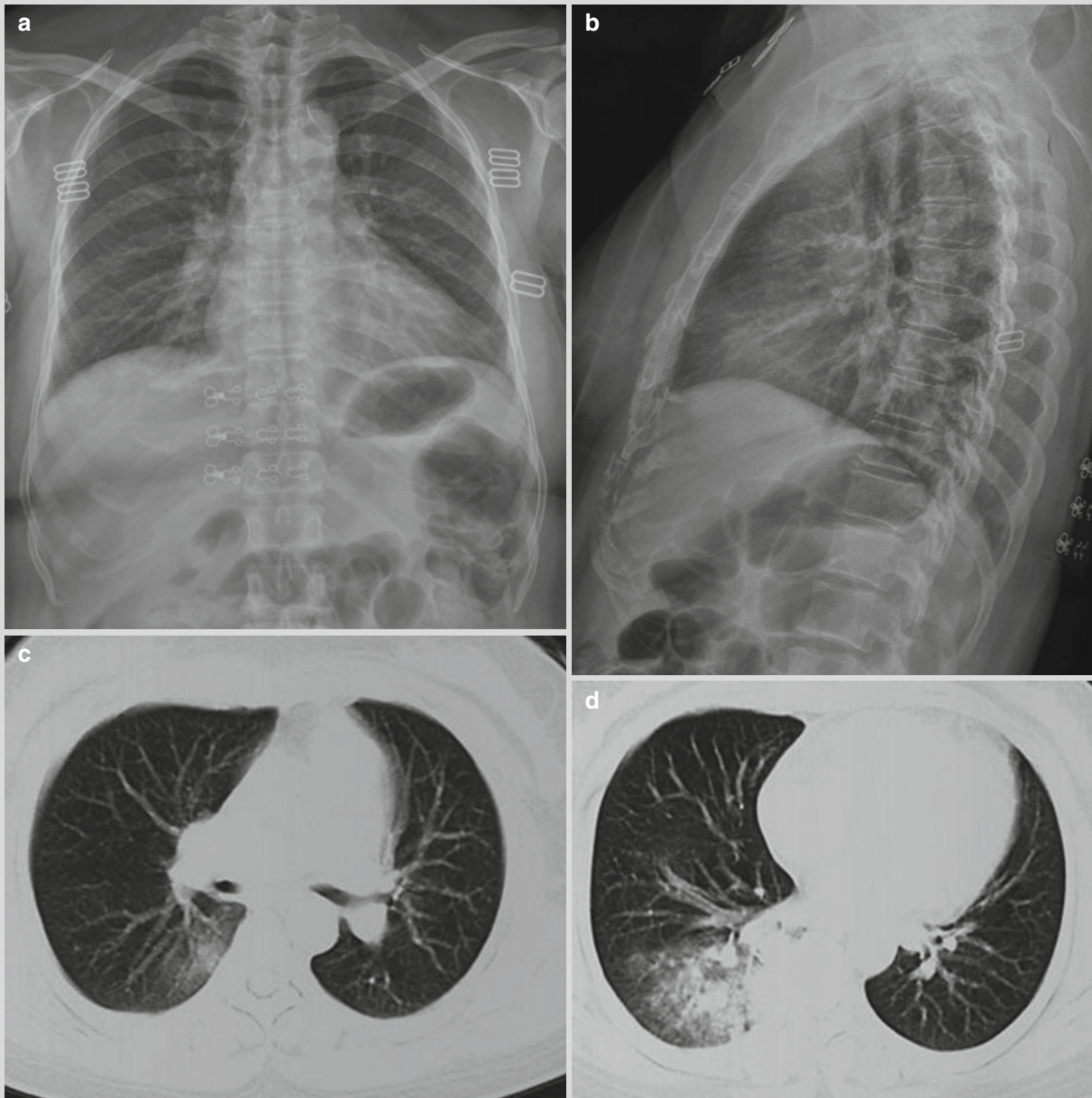


Fig. 11.11 On d 2 after onset, anterior-posterior and lateral X-ray showed poorly defined small flake of high density opacity near the cardiophrenic angle in the right lower lung field. And lateral X-ray demonstrated poorly defined small flake of opacity in the overlapping area of posterior costophrenic angle and thoracic vertebrae in the right lower lung field (**a**, **b**). On d 3 after onset, chest CT scan showed flake of ground glass opacity in the posterior basilar segment of right lower lung lobe (**c**). The right lower lung lobe was revealed with large flake of opacity with mixed GGO density and parenchymal density (**d**). On d 6 after onset, chest CT scan demonstrated large consolidation in the posterior basilar segment of right lower lung (**e**). The right middle

and lower lung was revealed with large consolidation with air bronchogram inside. The left lower lung was revealed with flake of consolidation and ground glass like high density opacity. Compared to the chest CT scan film 3 days ago, the lesions significantly progressed (**f**). On d 31 after onset, chest CT scan demonstrated absorbed consolidation opacity in the right lower lung lobe at the bronchial bifurcating level (**g**). The right lower lung lobe was revealed with GGO like opacity and interstitial fibrous cords like opacity near diaphragmatic dome. The left lingual lung lobe was revealed with GGO like opacity and interstitial fibrous cords like opacity (**h**)

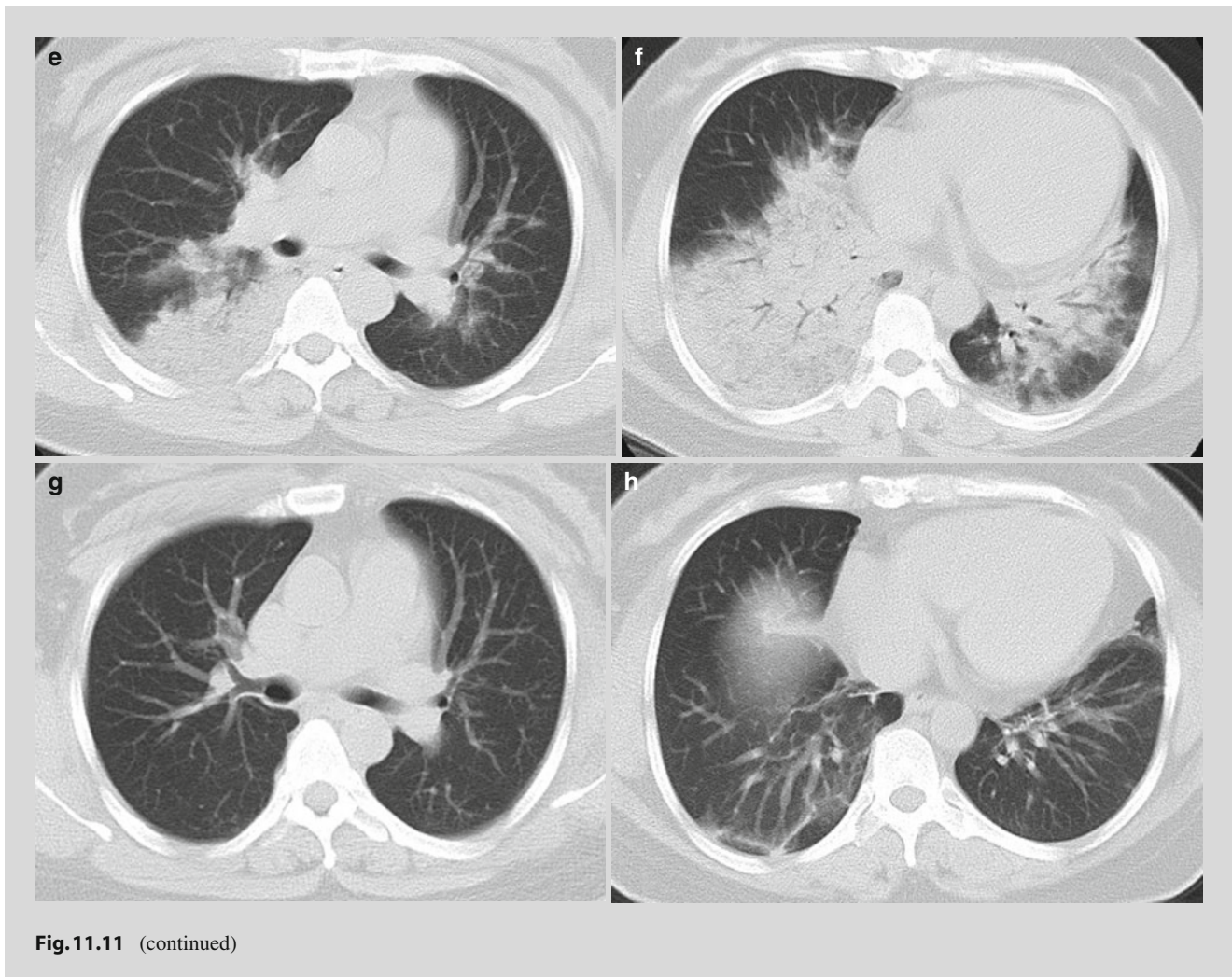


Fig.11.11 (continued)

References

- Ajlan AM, Quiney B, Nicolaou S, et al. Swine-origin influenza A(H1N1)viral infection: radiographic and CT findings. *AJR Am J Roentgenol.* 2009;193(6):1494–9.
- Cai RP, Du RB, Li T. Radiological demonstrations of lung lesions and their dynamic changes in human infected H7N9 avian influenza. *J Trauma Emerg (Electronic Version).* 2014;2(3):19–22.
- Chen Y, Liang W, Yang S, et al. Human infections with the emerging avian influenza A H7N9 virus from wet market poultry: clinical analysis and characterisation of viral genome. *Lancet.* 2013;381(9881):1916–25.
- Feng F, Jiang Y, Yuan M, et al. Association of radiologic findings with mortality in patients with avian influenza H7N9 pneumonia. *PLoS One.* 2013;9(4), e93885.
- Gao R, Cao B, Hu Y, et al. Human infection with a novel avian-origin influenza (H7N9) virus. *N Engl J Med.* 2013;368(24):1888–97.
- Huang XR, Huang H, Lu PX, et al. CT scan demonstrations and their relationship with virus load and CD4 T cell count in pneumonia induced by human infected H7N9 avian influenza. *J Radiol Pract.* 2014a;29(7):751–5.
- Huang XR, Zeng Z, Lu PX, et al. Radiological data analysis of pneumonia induced by human infected H7N9 avian influenza: report of 12 cases. *J CT MRI China.* 2014b;12(2):8–11.
- Li HJ. Recent understandings and insights about the emerging infectious disease: human infected H7N9 avian influenza. *Radiol Pract.* 2014;29(7):738–9.
- Li YF, Li HJ. Chest radiological demonstrations of human infected H7N9 avian influenza. *Radiol Pract.* 2014;29(7):745–7.
- Li L, Li HJ, Zhao J, et al. Chest radiological data of human infected H7N9 avian influenza: report of 13 cases. *Radiol Pract.* 2014;29(7):748–50.
- Lu PX, Zhou BP. Imaging diagnosis of emerging infectious diseases. Beijing: People's Medical Publishing House; 2013.
- Lu PX, Zeng Z, Zheng FQ, et al. Radiological demonstrations of severe pneumonia induced by human infected H7N9 avian influenza and their dynamic changes. *Radiol Pract.* 2014;29(7):740–4.
- National Health and Family Planning Commission of P.R.China. Clinical Guideline for human infected H7N9 avian influenza (2014). *Chin J Clin Infect Dis.* 2014;7(1):1–3.
- Song FX, Zhou J, Shi YX, et al. Bedside chest radiography of novel influenza A (H7N9) virus infections and follow-up findings after short-time treatment. *Chin Med J (Engl).* 2013;126(23):4440–3.
- Wang Q, Zhang Z, Shi Y, Jiang Y, et al. Emerging H7N9 influenza A (novel reassortant avian origin) pneumonia: radiologic findings. *Radiology.* 2013a;268(9):882–9.

- Wang Y, Zhou ZP, Zhang YW, et al. Clinical and radiological features of human infected H7N9 avian influenza. *Chin J Radiol.* 2013b;47(9):780-2.
- Wang YQ, Shi YX, Zhang ZY, et al. Primary radiological data analysis about pneumonia induced by human infected H7N9 avian influenza. *Chin J Radiol.* 2013c;47(6):505-8.
- Wang XM, Hu S, Hu CH, et al. Chest imaging of H7N9 subtype of human avian influenza. *Radiol Infect Dis.* 2015;1(2):51-6.
- Xin XY, Chang Y, Sun XM, et al. Chest radiological demonstrations of pneumonia induced by H7N9 avian influenza virus. *J Med Radiol.* 2015;47(9):637-40.
- Zeng Z, Lu PX, Zhou BP, et al. Radiological demonstrations of severe pneumonia induced by H7N9 avian influenza virus. *J Tubercu Lung Health.* 2014;3(1):25-8.
- Zhou BP, Li YM, Lu PX. *Human infected avian influenza.* Beijing: Science Press; 2007.